

1 **Zebrafish studies on the vaccine candidate to COVID-19, the Spike protein:**

2 **Production of antibody and adverse reaction**

3 Bianca H Ventura Fernandes^{1,32}, Natália Martins Feitosa², Ana Paula Barbosa³, Camila
4 Gasque Bomfim³, Anali M. B. Garnique⁴, Francisco I. F. Gomes^{5,6}, Rafael T.
5 Nakajima⁷, Marco A. A. Belo^{8,9}, Silas Fernandes Eto¹⁰, Dayanne Carla Fernandes¹¹,
6 Guilherme Malafaia¹², Wilson G. Manrique¹³, Gabriel Conde⁸, Roberta R. C. Rosales¹⁴,
7 Iris Todeschini¹⁵, Ilo Rivero¹⁶, Edgar Llontop¹⁵, German G. Sgro¹⁵, Gabriel Umaji
8 Oka¹⁵, Natalia F Bueno¹⁵, Fausto K. Ferraris¹⁷, Mariana T. Q. de Magalhaes¹⁸, Renata J.
9 Medeiros¹⁹, Juliana M. M Gomes²⁰, Mara de Souza Junqueira²¹, Katia Conceição²²,
10 Letícia G. Pontes²³, Antonio Condino-Neto²³, Andrea C. Perez²⁴, Leonardo J. G.
11 Barcellos^{25,26}, Jose Dias Correa junior²⁷, Erick G. Dorlass³, Niels O. S Camara²⁰, Edison
12 Luiz Durigon³, Fernando Q. Cunha^{5,6}, Rafael H. Nóbrega⁷, Glaucia M. Machado-
13 Santelli²⁸, Chuck Farah¹⁵, Flávio P Veras^{5,6}, Jorge Galindo-Villegas²⁹, Leticia Costa-
14 Lotufo³⁰, Thiago M. Cunha^{5,6}, Roger Chammas^{1,31}, Cristiane R. Guzzo³, Luciani R
15 Carvalho^{1,32}, Ives Charlie-Silva^{30*}

16

17 ¹Laboratório de Controle Genético e Sanitário, Diretoria Técnica de Apoio ao Ensino e
18 Pesquisa, Faculdade de Medicina da Universidade de São Paulo

19 ²Integrated Laboratory of Translational Bioscience (LIBT), Institute of Biodiversity and
20 Sustainability (NUPEM), Federal University of Rio de Janeiro (UFRJ)- Macaé, RJ,
21 Brazil.

22 ³Department of Microbiology, Institute of Biomedical Sciences, University of São
23 Paulo, São Paulo, Brazil.

24 ⁴Department of Cell Biology, Institute of Biomedical Sciences, University of São Paulo,
25 São Paulo, Brazil.

26 ⁵Center of Research in Inflammatory Diseases, Ribeirão Preto Medical School,
27 University of São Paulo, Ribeirão Preto, São Paulo, Brazil.

28 ⁶Department of Pharmacology, Ribeirão Preto Medical School, University of São Paulo,
29 Ribeirão Preto, São Paulo, Brazil.

30 ⁷Reproductive and Molecular Biology Group, Department of Morphology, Institute of
31 Biosciences, São Paulo State University, Botucatu, São Paulo, Brazil.

32 ⁸Department of Preventive Veterinary Medicine, São Paulo State University,
33 Jaboticabal, São Paulo, Brazil.

34 ⁹Laboratory of Animal Pharmacology and Toxicology, Brasil University, Descalvado,
35 São Paulo, Brazil.

36 ¹⁰Postgraduate Program in Health Sciences - PROCISA, Federal University of Roraima,
37 Brazil.

38 ¹¹Immunochemistry Laboratory, Butantan Institute, São Paulo, Brazil.

39 ¹²Biological Research Laboratory, Goiano Federal Institute – Urutaí Campus, GO,
40 Brazil.

41 ¹³Aquaculture Health Research and Extension Group - GRUPESA, Aquaculture Health
42 Laboratory - LABSA, Department of Veterinary Medicine, Federal University of
43 Rondônia, Rolim de Moura campus, Rondônia, Brazil.

44 ¹⁴Department of Cell and Molecular Biology, Ribeirão Preto Medical School,
45 University of São Paulo, Ribeirão Preto, São Paulo, Brazil.

46 ¹⁵Departamento de Bioquímica, Instituto de Química, Universidade de São Paulo,
47 Brazil.

48 ¹⁶Pontificia Universidade Católica de Minas Gerais

49 ¹⁷Department of Pharmacology and Toxicology, Oswaldo Cruz Foundation -
50 FIOCRUZ- Rio de Janeiro, Brazil.

51 ¹⁸Department of Biochemistry and Immunology, Institute of Biological Sciences – ICB,
52 Federal University of Minas Gerais, Belo Horizonte, Brazil.

53 ¹⁹Laboratory of Physiology - Zebrafish INCQS/Fiocruz Facility, Department of
54 Pharmacology and Toxicology – DFT, INCQS - National Institute for Quality Control
55 in Health. Rio de Janeiro, Brazil.

56 ²⁰Transplantation Immunobiology Lab, Department of Immunology, Institute of
57 Biomedical Sciences, Universidade de São Paulo, Brazil.

58 ²¹Center for Translational Research in Oncology, Cancer Institute of the State of São
59 Paulo, Faculty of Medicine, University of São Paulo, São Paulo. Brazil.

60 ²²Laboratory of Peptide Biochemistry, Federal University of São Paulo, Brazil.

61 ²³Laboratory of Human Immunology, Department Immunology, Institute Biomedical
62 Sciences, University Sao Paulo, Sao Paulo – Brazil.

63 ²⁴Department of Pharmacology, Universidade Federal de Minas Gerais, Brazil.

64 ²⁵Graduate Program of Pharmacology, Federal University of Santa Maria, Brazil.

65 ²⁶Laboratory of Fish Physiology, Graduate Program of Bioexperimentation and of
66 Environmental Sciences. University of Passo Fundo, Brazil.

67 ²⁷Laboratorio do Estudo da Interacao Quimico Biologica e da Reproducao Animal,
68 LIQBRA, Bloco O3,174, Departamento de Morfologia Instituto de Ciencias Biologicas,
69 Universidade Federal de Minas Gerais

70 ²⁸Department of Cell Biology, Institute of Biomedical Sciences, University of Sao
71 Paulo, Sao Paulo, Brazil.

72 ²⁹Faculty of Biosciences and Aquaculture, Nord University, 8049 Bodø, Norway

73 ³⁰Department of Pharmacology, Institute of Biomedical Sciences, Universidade de Sao
74 Paulo, Brazil.

75 ³¹Centro de Investigação Translacional em Oncologia, Instituto do Câncer do Estado de
76 São Paulo, Faculdade de Medicina da Universidade de São Paulo.

77 ³²Disciplina de endocrinologia do departamento de Clinica medica e Laboratório de
78 Hormônios e Genética Molecular, LIM 42

79

80 ***Corresponding author:**

81 Dr. Ives Charlie-Silva

82 e-mail: Charliesilva4@hotmail.com

83

84

85

86

87

88

89

90

91

92 **Summary**

93

94 Establishing new experimental animal models to assess the safety and immune response
95 to the antigen used in the development of COVID-19 vaccine is an imperative issue.
96 Based on the advantages of using zebrafish as a model in research, herein we suggest
97 doing this to test the safety of the putative vaccine candidates and to study immune
98 response against the virus. We produced a recombinant N-terminal fraction of the Spike
99 SARS-CoV-2 protein and injected it into adult female zebrafish. The specimens
100 generated humoral immunity and passed the antibodies to the eggs. However, they
101 presented adverse reactions and inflammatory responses similar to severe cases of
102 human COVID-19. The analysis of the structure and function of zebrafish and human
103 Angiotensin-converting enzyme 2, the main human receptor for virus infection,
104 presented remarkable sequence similarities. Moreover, bioinformatic analysis predicted
105 protein-protein interaction of the Spike SARS-CoV-2 fragment and the Toll-like
106 receptor pathway. It might help in the choice of future therapeutic pharmaceutical drugs
107 to be studied. Based on the *in vivo* and *in silico* results presented here, we propose the
108 zebrafish as a model for translational research into the safety of the vaccine and the
109 immune response of the vertebrate organism to the SARS-CoV-2 virus.

110

111

112

113

114

115

116

117

118

119

120

121

122

123

124

125

126 Introduction

127 The World Health Organization (WHO) registered, on January 30th, 2020, that
128 the outbreak of the disease caused by the severe acute respiratory syndrome coronavirus
129 2 (SARS-CoV-2) constituted a Public Health Emergency of International Importance
130 (the highest level of alert from the Organization)¹. Since then, the number of
131 Coronavirus Disease 2019 (COVID-19) cases outside China has increased significantly
132 worldwide, resulting in the deaths of approximately 1,108,000 of the nearly 40 million
133 infected people through October¹. The current coronavirus pandemic has had drastic
134 consequences for the world's population, not only in terms of the public health system
135 but also in causing a major global economic crisis. Diagnostic tests, efficient and safe
136 vaccines, and new effective antivirals are urgently required².

137 SARS-CoV-2 Spike protein is found on the surface of the virus, giving it a
138 “crown” appearance, and binds human (Homo sapiens) Angiotensin-converting enzyme
139 2 (ACE2) to infect human cells⁷. Moreover, the Spike protein is one of the likely
140 targets for vaccine production, and the antibodies against it could be used for SARS-
141 CoV-2 antigen rapid test production. To investigate the production of specific
142 antibodies against the Spike protein of SARS-CoV-2 in a zebrafish (*Danio rerio*) model,
143 we inoculated an N-terminal region of SARS-CoV-2 Spike recombinant protein
144 (residues 16-165) in adult female specimens. In humans, protection conferred by natural
145 infection or passive immunization are unclear¹. However, in teleost fish, including the
146 zebrafish, antibodies constitute a major proportion of the functional passive immunity
147 that is acquired maternally. Although maternal Abs are transferred to the fetus through
148 the placenta in mammals, in almost all teleost fish, Abs are transferred to the yolk². This
149 suggests that by injecting the recombinant spike protein abundant antibodies could be
150 obtained simply by extracting the antibodies from the eggs produced by a single adult
151 female zebrafish. The second goal of this work was to demonstrate that the zebrafish
152 could be a new alternative model to test preclinical vaccine candidates for COVID-19,
153 prospecting a strategy to assess safety and toxicity for vaccine candidates. The
154 comparison between zebrafish and human genomes revealed remarkable sequence and
155 functional conservation of 70% genetic similarity to humans^{3,4}. Zebrafish have been
156 used as a model to study the safety of vaccines⁵ and to assess toxicology that could be
157 correlated to human health^{6,7}. Recently, the WHO (2020) prepared a document on all
158 vaccine candidates for COVID-19 clinical trials, reporting 35 candidate vaccines in the

159 clinical evaluation and at least 166 vaccine candidates in preclinical and clinical
160 development. Normally, the development of a vaccine takes 10 to 15 years for
161 conclusion. However, the case of COVID-19 meets a new pandemic paradigm and the
162 development of the vaccine has been proposed to be reduced to 1-2 years⁸.

163 It is worth mentioning that before vaccine clinical tests begin, several safety
164 protocols must be submitted with *in vitro* and *in vivo* experiments on animal models.
165 There is a lack of information regarding the immune response of the organism to SARS-
166 CoV-2, including animal models to study it⁹. Although zebrafish do not have lungs as
167 humans do, the present study shows similar inflammatory responses observed in severe
168 cases of COVID-19 patients that could be considered when investigating human
169 responses to the virus.

170 In the global task to develop the vaccine and possible therapeutic approaches for
171 COVID-19, several animal models have been proposed, such as mice¹⁰, hACE2
172 transgenic mice¹¹, alpaca¹², golden Syrian hamsters, ferrets, dogs, pigs, chickens, and
173 cats⁹, and species of non-human primates¹⁰. Recently, three reports have described the
174 production of equine neutralizing antibodies against SARS-CoV-2^{13,14}. A study by Deng
175 and collaborators analyzed serum samples from 35 animal species for the detection of
176 specific antibodies against SARS-CoV-2¹⁵. Despite this wide search for candidate
177 animal models, so far only two references promote the zebrafish model on this regard
178 confirming the innovative and pioneer characteristics of our study^{16,17}.

179 Here, female zebrafish individuals injected with a N-terminal fraction of SARS-
180 CoV-2 Spike recombinant protein (residues 16-165) produced specific antibodies, and
181 presented suggestive adverse reactions and inflammatory responses resembling the
182 severe cases of COVID-19 human patients. Therefore, with this work we put forward
183 the advantage of using zebrafish as a model for translational research on the vaccine
184 safety and the screening of immune response against the SARS-CoV-2 virus.

185

186 **Results**

187 **Humoral immune response of zebrafish immunized with N-terminal fraction of** 188 **rSpike protein**

189 To induce and analyze the humoral immune response, 3 peptides of full length
190 SARS-CoV-2 Spike were generated after a pattern memorizing phagolysosomal
191 proteolysis using the virtual proteolytic cleavage tool (Figure 1a and 1a.1). One of them,

192 the peptide named Pep1 (Pep1, residues 16 to 22; Pep2 and Pep3 are shown in
193 Supplemental Figure 1) (Figure 1a-a2), has been chosen because of its promising
194 antigenic potential. It has presented a binding free energy site in protein-ligand
195 interactions for *D. rerio* MHC II, MHC I, TCR alpha (Figure 1b). Similar results were
196 observed when the same analysis was performed using human orthologous receptors
197 (Figure 1b). Further analysis were carried out based on Dock analysis between Pep15
198 and the structure of MHC II (PDBID), MHC I (PDBID), TCR alpha (PDBID), and TCR
199 beta (PDBID) that showed the similarity of the ligand/Pep1 interaction to the receptor-
200 binding site (Figure 1c). After the *in silico* examination, specific pathogen free wildtype
201 (AB SPF) adult female zebrafish were injected with a N-terminal fragment of SARS-
202 CoV-2 Spike protein (residues 16 to 165) expressed in *Escherichia coli* with a N-
203 terminal fusion of six histidine tag and purified from inclusion bodies, herein name
204 rSpike, to determine whether they could produce IgM-class antibodies. In 7 days of
205 immunization, a band corresponding to IgM in the plasma was detected using SDS-
206 PAGE and was also and analyzed by MALDI-ToF. It was two-fold higher than the
207 controls (Figure 1e, g). After 7 days a new immunization using rSpike was done and the
208 IgM level remained higher than the control after 14 days being more evident in IgM of
209 eggs (Figure 1e, g).

210 Docking analysis showed that the zebrafish IgM chain 4 (CH4) share 43.3%
211 sequence similarity to human IgM CH4 (Figure 1d) and might have similar potential to
212 recognize S protein as the human antibody. In parallel, it was tested whether passive
213 antibody transfer to the eggs occurred through immunized females. The bands
214 corresponding to the size of IgM in unfertilized zebrafish eggs were detected in the gel
215 (Figure 1f) and confirmed by protein analysis with MALDI-ToF. It was possible to
216 observe an increase in IgM in eggs compared to the control after 7 days, and it was
217 almost two-fold higher after 14 days of maternal immunization (Figure 1h).

218

219 **rSpike protein immunization of zebrafish had an impact on the survival rate**

220 Two bioassays were carried out to analyze the toxicity of the rSpike. Although
221 the immunized fish produced antibodies, the first injection of the rSpike generated high
222 toxicity to the fish (Figure 2). Therefore, the assay was repeated by adding different

223 control groups to confirm that the toxicity findings were specific to the rSpike (Figure
224 2). In the first bioassay, after fish immunization with rSpike, the survival rate was
225 78.6% during the first seven days (Figure 2). It was significant when compared to naive
226 control and fish injected with protein buffer (control 1), where the survival rate was
227 100% and 90%, respectively (Figure 2). Nonetheless, after a second immunization, the
228 rSpike immunized group maintained the plateau survival rate, with no statistical
229 significance between the groups for the relative risk of death (Figure 2).

230 Therefore, a second assay was conducted by adding different control groups in
231 order to confirm that the toxicity findings were specific to the rSpike, and related to the
232 presence of any antigen. The Kaplan-Meier survival analysis confirmed rSpike injection
233 presented a lower survival rate compared to the two previous controls used (Control
234 naïve and protein buffer) and also compared to females injected with *E. coli* extract or a
235 culture medium mixed of two purified recombinant proteins (PilZ protein from
236 *Xanthomonas citri*, and a N-terminal fragment of LIC_11128 from *Leptospira*
237 *interrogans* Copenhageni) (Control 2) (Figure 2). The survival rate was maintained after
238 the second immunization for the next seven days. The relative risk of death in the period
239 studied between the groups was significant (chi square = 79.70; $p < 0.0001$).

240

241 **rSpike protein produced an inflammatory response and critical damage in** 242 **different tissues of adult zebrafish**

243 In order to verify the occurrence of sublethal effects of the rSpike on treated
244 zebrafish, histopathological analysis of different organs, including brain, gonads, heart,
245 kidney, liver, spleen, among others, was performed in female fishes used in the
246 immunization protocol described in material and methods. Animals that died during the
247 immunization experiment were excluded from the analysis. In general, it was observed
248 several morphological alterations compatible with an undergoing inflammatory process
249 in many tissues. Markedly, brain obtained from treated fishes showed an intense
250 inflammatory infiltrate with presence of many macrophages after 7 days (Figure 3c) and
251 an intense mononuclear infiltrate after 14 days (Figure 3d,e). Histopathological analysis
252 of the female reproductive tissue showed ovarian stroma with abundant and
253 disorganized extracellular matrix (Figure 3g). Follicular development showed

254 alterations such as atresia among oocytes at primary growth and cortical alveolus stages
255 (Figure 3g). Moreover, dense inflammatory infiltrates are commonly seen in the ovarian
256 stroma (Figure 3h). On the other hand, the group of fish that received a second injection
257 within the interval of 7 days showed no histological changes in their ovaries after 14
258 days, when compared to controls (Figure 3i). In kidneys, we observed melanin and
259 lipofuscin pigments, renal thrombosis and autophagy with tubular disarray and loss of
260 tubular lumen epithelium, loss of Bowman's capsule space and the integrity of the
261 glomerular tuft compromising blood filtration (Figure 3n,o). The frequency of the
262 relative systemic alterations is summarized in Table 1.

263

264 **rSpike protein immunization induces systemic neutrophils and macrophage** 265 **infiltration in zebrafish**

266 Taking together clinical evidences of the immunological effects of rSpike
267 protein and the inflammatory-related alterations in the architecture of treated zebrafish
268 tissue, we then turn to a more detailed investigation of the activation of the immune
269 system upon injection of rSpike protein in zebrafish. The presence of the major
270 inflammatory cells as neutrophils and activated macrophages present in the brain and
271 coelomic cavity of the zebrafish were detected by immunostaining. Antibodies against
272 Lymphocyte antigen 6 complex locus G6D (Ly6G), and Allograft inflammatory factor 1
273 (AIF-1/Iba1) were used to identify neutrophils and activated macrophages, respectively.
274 In non-immunized fish (control group), there was no visible staining for AIF-1/Iba1
275 (Figure 4 - panel a3); but there was weak staining for Ly6G in the nervous system and
276 ventral area of the coelomic cavity (Figure 4 panel a4). However, the females injected
277 with rSpike protein presented strong Ly6G and AIF-1/Iba1 staining, indicating an
278 inflammatory response of the organism to the virus protein (Figure 4b). Colocalization
279 between Ly6G and AIF-1/Iba1 was observed with predominance in the peripheral
280 region of the brain and in the portion of the kidney from the head (Figure 4b, field 1).
281 Macrophages and neutrophils were also labeled in large vessels (Figure 4b, field 2). In
282 the coelomic cavity in general, there was an increase of neutrophil (Ly6G) and
283 macrophage (AIF/Iba1) cell infiltration (Figure 4c).

284 The innate immune system and antibody production were detected after rSpike
285 injection in adult zebrafish. The question remained as to whether the fish could respond

286 through cellular immunity, especially T cells. To answer this question, immunostaining
287 revealed the presence of CD-4 and CD-8 cells in the coelomic cavity of female adult
288 zebrafish injected with rSpike (Figure 5).

289

290 **The human receptor Angiotensin converting enzyme 2 (ACE2) share 72%** 291 **sequence similarity to its ortholog in zebrafish**

292 One of the known targets of SARS-CoV-2 Spike protein is the Angiotensin
293 receptor converting enzyme 2 (ACE2) in humans. It is considered the main gateway to
294 the virus infection. Considering the effects of rSpike protein on the fishes analyzed in
295 this work, structural and functional similarities between zebrafish and human ACE2
296 were investigated, using bioinformatic analysis. Interestingly, zebrafish has ACE2
297 protein that shares 58 and 72 % primary sequence identity and similarity to human
298 ACE2, respectively (Figure 6; Supplemental Figure 2). Human ACE2 interacts to the
299 receptor binding domain (RBD) of SARS-CoV-2 Spike protein mainly by polar and salt
300 bridge interactions. Human ACE2 has 22 residues making part of the protein-protein
301 interaction and most of them are located at the N-terminal region of ACE2. 77% of the
302 human ACE2 residues of the interface are similar in zebrafish ACE2 sequence (Figure
303 6; Supplemental Figure 2) suggesting that zebrafish may also binds SARS-CoV-2 Spike
304 protein. The tree-dimensional structure of zebrafish ACE2 based on homology model
305 (Figure 6a) shows a high structural similarity with human ACE2. Computational
306 analysis of protein-protein interaction using ACE2 and the RBD of SARS-CoV-2 Spike
307 protein reveals similar values of binding free energy suggesting that zebrafish is
308 susceptible to virus infection (Figure 6c). In our work, we do not expect that rSpike
309 protein interacts with zebrafish ACE2 because rSpike correspond to the N-terminal part
310 of the Spike protein (residues 16-165) that precedes the RBD domain (residues 319-
311 541).

312

313 **The protein-protein interaction prediction among SARS-CoV-2**

314 The protein-protein interaction prediction among the rSpike and zebrafish
315 proteins according to the subcellular location (membrane, cytoplasm, and nucleus)
316 predicted interactions with 2,910 proteins for the membrane, 771 proteins for the

317 cytoplasm, and 1,134 proteins for the nucleus (Table 2; Supplementary Table 1). For
318 human proteins and rSpike predicted interactions with 1,785 proteins for the membrane,
319 1,168 proteins for the cytoplasm, and 1,242 proteins for the nucleus (Table 2;
320 Supplementary Table 1). Considering the most general ontological terms found
321 hierarchically, according to the KEGG and Reactome databases, 71% of the terms
322 identified for zebrafish are identical to those found for human. However, further
323 analysis showed different specific terms with approximately 58% of different specific
324 pathways.

325 Functional enrichment of the biological pathways (zebrafish and human) showed
326 basic processes related mainly to cell growth and death, including regulation of
327 transcription and translation mechanisms, mechanisms of DNA repair or replication,
328 and signaling pathways of p53 and by GPCR, among others. Additionally, we identified
329 the pathways related to signal molecules and interactions, signal transduction, and the
330 immune system (Figure 7, Supplementary Table 1).

331 Interestingly, it was recovered through the protein-protein interaction with
332 rSpike, the Toll-like receptor pathway (dre:04620 and hsa:04620). It can allow
333 interaction with the Toll-like receptors TLR1, TLR2, TLR4, and TLR5 and the
334 interferon- α/β receptor (IFN $\alpha\beta$ R), possibly triggering the activation of various signaling
335 pathways (Figure 8). In this pathway, we observed a possible interaction of the rSpike
336 with the signal transducer and activator of transcription 1-alpha/beta (STAT1) protein in
337 the cytoplasmic region. Additionally, the signal molecules and interaction pathway
338 (zebrafish and human) showed the possibility of rSpike interacting with a considerable
339 number of cell receptors related to the neuroactive ligand receptor (KEGG:4080) and a
340 cytokine-cytokine receptor (Figure 8, KEGG:4060) and triggering diverse cellular
341 signaling such as the TGF beta signaling family, class I and II helical cytokines, IL and
342 TNF family. In addition, proteins related to the extracellular matrix, cellular
343 communication and motility, formation of vesicles, transport and catabolism, VEGF
344 signaling pathway, and AGE-RAGE signaling pathway in diabetic complications,
345 among others, were identified (see Supplementary Table 1).

346 The possible virus-host protein interactions during the SARS-CoV-2 infection
347 were tested in network analysis based on protein interactions (Figure 9). The important
348 similarity between SARS-CoV-2 proteome and SARS-CoV proteome¹⁸ allowed us to

349 hypothesize that the SARS-CoV proteome is highly conserved in SARS-CoV-2. In our
350 network analysis we were able to detect 29 proteins (Figure 9). A PPI interaction
351 database was assembled, including 7 nodes and 29 interactions. We analyzed the
352 following proteins: Parvalbumin 4 (Pvalb4), Creatine kinase (Ckma), Keratin 5 (Krt5),
353 A kinase anchor protein 1 (Ak1), Malate dehydrogenase (Mdh1aa), 2-phospho-D-
354 glycerate hydro-lyase (Eno3), Component Chromosome 15 (ENSDARG00000095050),
355 Component Chromosome 1 (wu:fk65c09), Component Chromosome 16 (Zgc:114037),
356 Component Chromosome 17 9 Zgc:114046), Component Chromosome 26
357 (ENSDARG00000088889), Apolipoprotein A-II (Apoa2), Apolipoprotein A-Ib
358 (Apoa1b), Serpin peptidase inhibitor member 7 (Serpina7), Transmembrane serine
359 protease 2 (tmprss2), Fetuin B (fetub), Apolipoprotein A-I (apoa1a), Carboxylic ester
360 hydrolase (ces3), Apolipoprotein Bb (apobb), tandem duplicate 1, Fibrinopeptide A
361 (fga), Serotransferrin (tfa), Apolipoprotein C-I (apoc1), Complement component C9
362 (c9), Pentaxin (crp), Ceruloplasmin (cp), Hemopexin (hpx), Bal protein (bal),
363 Component Chromosome 13 (ENSDARG00000), and Component Chromosome 25
364 (ENSDARG0000008912).

365

366 **Discussion**

367 Here we show, for the first time, that zebrafish injected with rSpike protein,
368 fragment 16 to 165 (rSpike), that corresponds to the N-terminal portion of the protein,
369 produced an acquired and native immune response and showed adverse effects,
370 following a series of experiments to validate a model of pre-clinical safety studies.

371 The first experiments aimed to analyze the humoral response with antibody
372 production and used, besides the rSpike, the appropriate negative controls as the *E. coli*
373 extract, mixed of purified recombinant proteins from bacteria, and buffer without the
374 virus protein. There was no increased in computed densitometry of the fragment related
375 to the IgM production in the control groups. Interestingly, the fragment was found only
376 in animals injected with rSpike, demonstrating the specificity of the immune response.
377 Despite the zebrafish systemic antibody production after day 7 of injection of rSpike,
378 the efficiency of these antibodies may have increased on the 14th day, conferring a
379 reduction in the mortality rate of the immunized animals. It was observed using SDS-
380 PAGE that a suggestive time-dependent increase of the fragment correlated with the

381 molecular weight of IgM in zebrafish serum. The results observed in the production of
382 antibodies at 7 and 14 days after inoculation also suggest the similarity to human
383 infected individuals with COVID-19¹⁹. Antibody production was found in the serum,
384 and in the eggs as well (Figure 1).

385 In the literature, the passive transfer of antibodies to eggs is known in zebrafish
386 and other teleosts²⁰. It has also been described as a strategy for immunization in
387 aquaculture to farmed fish². In evolution, the passive transfer of antibodies protects the
388 offspring from fish to mammals, along with other groups of tetrapods^{2,21}. Although in
389 mammals, the IgG is transferred through the placenta and breast milk, in fish the IgM
390 plays this role in the yolk²¹. Similarly, in humans, the presence of SARS-CoV-2
391 antibodies in breast milk has been found to provide passive immunity for children, to
392 protect them^{22,23}. In this sense, the antibody transfer shown in zebrafish could be helpful
393 in future studies to understand the maternal immunological protection of descendants
394 against SARS-CoV-2 or any other vaccine candidates. Also, measuring antibodies
395 against the rSpike in plasma and egg demonstrates great potential for the use of
396 zebrafish in the early stages (phases I and II) of the development and use of these
397 antibodies in therapeutics and prophylactics for humans^{24,25}.

398 Interestingly, fish injected with rSpike produced a toxic inflammatory response
399 with similarity to severe cases of COVID-19 in humans (Figure 2 and 3). Different
400 systems were affected, including the nervous system. The first hint of rSpike toxicity
401 was the distinct swimming behavior that adult females presented after the protein
402 injection. In fact, some recent studies have reported that the SARS-CoV-2 may affect
403 the nervous system²⁶⁻²⁸ as the peripheral nervous system²⁹⁻³¹, particularly in the most
404 severe cases of infection³².

405 In our study, the rSpike was responsible for generating an inflammatory process
406 in the brain, characterized by an intense influx of mononuclear cells, but no
407 histopathological lesions. This profile is in line with the clinical reports of COVID-19-
408 associated acute necrotizing myelitis³³, where lymphocytic pleocytosis was observed in
409 the cerebrospinal fluid (CSF). Acute transverse myelitis related to SARS-CoV-2
410 infection²⁴, where an intense leukocyte infiltrate of monocytic characteristic and
411 elevated protein level was also observed in the CSF. In another report, thrombosis in
412 superficial and deep systems, straight sinus, the vein of Galen, internal cerebral veins,

413 and thrombosis of the deep medullary veins were found²⁷. Damage to the structure and
414 function of this system can lead to severe encephalitis, toxic encephalopathy, and, after
415 viral infections, severe acute demyelinating lesions³⁴. In a case study of 4 children with
416 COVID-19, Abdel-Mannan and collaborators reported that children with COVID-19
417 may have late neurological symptoms³⁵. Future studies with zebrafish might provide
418 more information about the virus damage in the nervous system.

419 To date, we do not know how the rSpike can cause neurological effects. It is
420 possible that the immune system can recognize these sequence of amino acids. The *in*
421 *silico* analysis of the rSpike used in the present study indicated that it might interact in a
422 protein-protein level with the Toll-like receptor pathway. In this pathway, the Jak/Stat
423 signaling in humans has been demonstrated to be activated in response to SARS-CoV-2
424 infection by the release of interleukin IL-6^{36,37}. Interestingly, our prediction showed the
425 possible interaction of the rSpike with the signal transducer and activator of
426 transcription 1-alpha/beta (STAT1) protein in the cytoplasmic region, which acts as a
427 carrier for the nucleus and, consequently, executes its function in the inflammatory
428 response as a transcription factor³⁸⁻⁴⁰. In addition, a study in mice showed that STAT1
429 deficiency did not affect the response of EGF and other cytokines such as IL10.
430 However, STAT1-deficient mice are more susceptible to pulmonary mycobacterial
431 infection⁴¹. Similarly, we observed the possibility of interaction with the extracellular
432 signal-regulated kinase 1/2 protein (ERK), in the zebrafish pathway, that plays a role in
433 signaling cascades and produces extracellular signals to intracellular targets⁴².

434 The response to SARS-CoV-2 in humans appears to be hemophagocytic
435 lymphohistiocytosis (HLH), characterized by immune hyperactivation that occurs when
436 Natural Killer cells and cytotoxic T lymphocytes do not eliminate activated
437 macrophages, leading to excessive production of pro-inflammatory cytokines⁴³. These
438 pro-inflammatory cytokines could be associated with a major pathomechanism in
439 kidney damage causing nephrotic proteinuria, collapsing glomerulopathy, membranous
440 glomerulopathy, nephritis, and acute tubular injury⁴⁴. Although some data suggest the
441 incidence of Acute Kidney Injury (AKI) by SARS-CoV-2 to be low^{45,46}, other studies
442 indicate that AKI is one of the significantly more common complications in patients
443 who died of COVID-19, pointed out as a marker of multiple organ dysfunction and
444 severe disease⁴⁶⁻⁴⁸.

445 Although we did not measure this cytokine storm, we were able to observe
446 significant renal alterations in the injected animals. In addition, we observed an increase
447 of lymphocyte levels and an increase in melanin and mipofuscin in the kidneys that
448 could be associated with an intense activation of the immune system cells due to the
449 rSpike immunizations response, associated with the accumulation of immune
450 complexes⁴⁹. These results suggest that the immunized fish produced immune
451 complexes.

452 Histological alterations were analyzed in the liver as mild lobular infiltration by
453 small lymphocytes, centrilobular sinusoidal dilation, patchy necrosis, moderate
454 microvesicular steatosis, mild inflammatory infiltrates in the hepatic lobule, and the
455 portal tract. These changes are similar to those observed in patients with COVID-19^{31,48}.
456 Although the zebrafish biochemical liver function was not tested, a three-fold increase
457 in ALT, AST, and GGT levels has been reported during hospitalization⁴⁸. These
458 alterations could be due to the direct cytopathic effect of the virus and could be
459 associated with higher mortality⁵⁰.

460 With respect to the reproductive tissue, female zebrafish injected with rSpike
461 displayed severe damage in the ovary (follicular atresia, cellular infiltration, and
462 disorganized extracellular matrix) after 7 days of protein inoculation. On the other hand,
463 it is remarkable that ovarian damage was reversed after 14 days, when zebrafish
464 received a second injection of rSpike. In humans, there is evidence that ACE2 mRNA is
465 expressed, at low levels, during all stages of follicle maturation in the ovary⁵¹, and also
466 in the endometrium⁵². This pattern of ACE2 expression, in line with our observations,
467 could suggest that SARS-CoV-2 affects female fertility in humans and zebrafish. More
468 studies will be necessary to comprehend the molecular mechanisms underlying SARS-
469 CoV-2-induced female infertility and the effects in the ovarian function. To date,
470 damage in the female reproductive system of COVID-19 patients has not been reported
471 yet⁵³.

472 In the sequence of these experimental findings, the *in silico* analysis showed
473 that zebrafish Ace2 receptor has the same potential for protein-ligand interaction as in
474 humans (Figure 6). We show *in silico* and *in vivo* that the zebrafish Ace2 receptor is
475 susceptible to the rSpike and interacts similarly to the human ACE2 receptor. The
476 importance of ACE2 receptor for SARS-CoV-2 infection and its role in vaccine studies
477 is shown in research with transgenic mice (HFH4-hACE2 in C3B6 mice)⁵⁴. The use of

478 ACE2 receptor by SARS-CoV-2 in the attachment and infection of the host cells has
479 been well postulated in mammals, except for murines, and some birds, such as
480 pigeons⁵⁵. The ACE-2 orthologue studies in non-mammalian animals, including
481 zebrafish, suggest the potential to unveil the role of this enzyme and its use for
482 therapeutic purposes⁵⁶.

483 The receptors associated with the zebrafish humoral and cellular immune
484 response showed structural and functional homology with the human MHC II, MHCI,
485 TCR alpha and beta receptors. Similar results were observed by Bhattacharya and
486 collaborators, who analyzed by docking interaction of 13 peptides with the human MHC
487 I and II receptors and observed the antigenic capacity of these peptides⁵⁷. Our findings
488 provided functional similarity of the same receptors in zebrafish, showing the
489 immunogenic capacity of the alpha and beta TCR receptors, and the functional
490 similarity with the human receptor. The *in silico* data can recognize, process, and
491 present antigens associated with rSpike protein that might be validated in *in vivo* studies
492 in future (Figure 1 a-d). As in mammals, the zebrafish has a conservative adaptive
493 immune system composed of T and B lymphocytes that develop from the thymus and
494 kidneys, respectively. The conservation of the immune system through evolution
495 reveals the importance of fish immunology studies to improve our knowledge of
496 mammalian immunity^{58,59}.

497 The zebrafish enzymatic system is involved in the genetic rearrangement process
498 in which B (BCR) and T lymphocyte receptors (TCR) originate. They also have, like
499 humans, recombinant activating genes that control the gene segments V, D, and J,
500 producing a diversity of antibodies and lymphocyte receptors⁶⁰. Despite this, teleosts
501 produce only three classes of antibodies: IgM⁶¹, IgW⁶², and IgZ, the latter exclusive to
502 zebrafish⁶³. Studies in zebrafish showed that in the regions of the BCR receptor were
503 targets of mutations⁵. Although the affinity of antibodies in ectothermic vertebrates is
504 less efficient than in mammals, the deaminase activation and affinity maturation might
505 contribute to the diversification of antibodies in zebrafish^{64,65}.

506 The world is now experiencing a global campaign to propose and test
507 therapeutics and vaccines. It is imperative to identify animal models for COVID-19 that
508 provide a translational approach for possible successful interventions. From February to
509 October 2020, the findings with animal models for COVID-19 included several

510 candidates, such as mice, Syrian hamsters, ferrets, non-human primates, minks, cats,
511 dogs, pigs, chicken, ducks, and fruit bats⁶⁶. However, no references regarding zebrafish
512 models were found.

513 Finally, the conserved genetic homology between zebrafish and humans⁴ might
514 be one of the reasons for the intense inflammatory reaction from the immune system of
515 zebrafish to rSpike analyzed in this work. It has provoked damage to organs in a similar
516 pattern as happen in severe cases of COVID-19 in humans. The fish produced innate
517 and acquired immunity that is suitable for future studies to gather valuable information
518 about vaccine responses and therapeutic approaches. Altogether, we present the
519 zebrafish as an animal model for translational COVID-19 research.

520

521 **Declaration of Competing Interest**

522 The authors declare that they have no competing interests.

523

524 **Acknowledgments**

525 Financial and material support was provided through the São Paulo Research
526 Foundation (FAPESP) granted to: Ives Charlie: Fapesp #2018/07098-0; 2019/19939-1;
527 Cristiane Rodrigues Guzzo: Fapesp #2019/00195-2, 2020/04680-0; Chuck Farah:
528 Fapesp #2017/17303-7; Germán G. Sgro: Fapesp #2014/04294-1; Edgar E. Llontop:
529 Fapesp #2019/12234-2; Natalia F. Bueno: Fapesp #2019/18356-2; Camila G. Bomfim:
530 Fapesp #2019/21739-0. LJGB is supported by a research fellowship from Conselho
531 Nacional de Desenvolvimento Científico e Tecnológico, Brazil (CNPq) 303263/2018-0
532 and FIGG has a PhD fellowship from FAPESP (2019/14285-3). We would like to thank
533 the Medical School Foundation for financial support (Project CG 19,110). We would
534 also like to thank the entire organizing team of the Global Virtual Hackathon 2020 for
535 the award our team received and the support from the Ministry of Transport,
536 Communications and High Technologies of the Republic of Azerbaijan, the United
537 Nations Development Program, and the SUP.VC Acceleration Center. Authors are also
538 thankful to Sartorius for technical support in this work.

539

540 **Materials and methods**

541 **Zebrafish maintenance**

542 Wild-type zebrafish from the AB line, and specific pathogen-free (SPF), were
543 raised in Tecniplast Zebtec (Buguggiate, Italy) and maintained in the zebrafish housing
544 systems in the XXXXXXXXXXXXXXXXXXXX facilities. Fish used for the experiments were
545 obtained from natural crossings and raised according to standard methods⁶⁷. Zebrafish
546 were kept in 3.5 L polycarbonate tanks and fed three times a day with Gemma micro by
547 Skretting (Stavanger, Norway). The photoperiod was 14:10 hours light-dark cycle and
548 the water quality parameters were 28°C ± 2°C; pH = 7.3 ± 0.2; conductivity 500 to 800
549 µS/cm, referred to as system water. The procedures were approved by the Ethics
550 Committee (CEUA) of the XXXXXXXXXXXXXXXXXXXXXXXXXXXXXXXXXXXX and registered
551 under protocol number XXXXXXXXX.

552

553 **Production of recombinant Spike Protein SARS-CoV-2 antigen-based vaccines**

554 Cloning, protein expression, and purification. The DNA fragment coding for the
555 SARS-CoV-2 Spike protein fragment from 16 to 165 (rSpike) was amplified by PCR
556 using SARS-CoV-2 cDNA transcribed from the RNA isolated from the second
557 XXXXXXXXXXXXXX patient, strain HIAE-02:SARS-CoV-2/SP02/human/2020/BRA
558 (GenBank accession number MT126808.1) provided by
559 XXXXXXXXXXXXXXXXXXXXXXXXXXXX. The primers used for amplification of the Spike
560 fragment are 5' AGCATAGCTAGCGTTAATCTTACAACCAGAACTCAATTACC 3'
561 and 5' ATTATCGGATCCTTAATTATTCGCACTAGAATAAACTCTGAAC 3'. The
562 PCR product was purified using the GeneJET PCR Purification Kit (Thermo Fisher
563 Scientific) and digested with Anza™ restriction enzymes *NheI* and *BamHI* (Thermo
564 Fisher Scientific). The expression vector used was pET-28a that was also digested with
565 the same pair of restriction enzymes as the amplified rSpike DNA fragment. The
566 digested fragment was used to ligate the rSpike DNA fragment to the digested pET-28a
567 vector using T4 DNA ligase (Thermo Fisher Scientific). The positive clones were
568 confirmed by digestion tests. The rSpike cloned into pET28a results in a protein with a
569 fusion of seven histidine tag at the N-terminal portion of the protein to facilitate the
570 protein purification steps.

571 rSpike was expressed in *Escherichia coli* strain BL21(DE3) and BL21(DE3)
572 Star. The cells were grown in 2XTY medium (16 g/L of bacto-tryptone, 10g/L of yeast

573 extract, and 5g/L sodium chloride) with added kanamycin (50 µg/ml) under agitation of
574 200 rpm at 37°C to an OD_{600nm} of 0.6, at which point 0.5 mM isopropyl-β-D-1-
575 thiogalactopyranoside (IPTG) was added. After 4 hours of induction, the cells were
576 collected by centrifugation and stored at 193 K. The cell pellet expressing the rSpike
577 protein was resuspended in lysis buffer (50 mM Tris-HCl pH 7.5, 200 mM NaCl, 5%
578 glycerol, 0.03% Triton-100 and 0.03% Tween-20) and lysed by sonication on an ice
579 bath in a Vibracell VCX750 Ultrasonic Cell Disrupter (Sonics, Newtown, CT, USA).
580 The lysate was centrifuged at 30.000 x g, 4°C for 45 minutes. The pellet fraction was
581 resuspended in 7M urea, 50 mM Tris-HCl pH 7.5, 200 mM NaCl, and 20 mM imidazole
582 on an ice bath under agitation for one hour and centrifuged at 30.000 x g, 4°C for 45
583 minutes. The soluble fraction was loaded in a HisTrap Chelating HP column (GE
584 Healthcare Life Sciences) previously equilibrated with 7M urea, 50 mM Tris-HCl pH
585 7.5, 200 mM NaCl, and 20 mM imidazole. Bound proteins were eluted using a linear
586 gradient of imidazole over 20 column volumes (from 20 mM to 1 M imidazole).
587 Fractions with rSpike were concentrated using Amicon Ultra-15 Centrifugal filters
588 (Merck Millipore) with a 3 kDa membrane cutoff and loaded onto a HiLoad 16/600
589 Superdex 75 pg (GE Healthcare Life Sciences) size exclusion chromatography column
590 previously equilibrated with 7M urea, 50 mM Tris-HCl pH 7.5, 200 mM NaCl, and
591 1mM EDTA. The eluted fractions containing rSpike protein were analyzed by 15%
592 SDS-PAGE for purity, and the fractions with the target protein were mixed and
593 concentrated using Amicon Ultra-15 Centrifugal filters (Merck Millipore) with a 3 kDa
594 membrane cutoff (Figure 10).

595

596 **The immunization administration**

597 We performed 2 intraperitoneal (IP) inoculations of a solution containing 1 µg
598 purified rSpike diluted in 10 µL of inoculation buffer (7M urea, 50 mM Tris-HCl pH
599 7.5, 200 mM NaCl, and 1mM EDTA). A group of control animals received injections
600 containing only the dilution buffer. Another control group was challenged by a lysate of
601 bacterial fragment of *E. coli* BL21(DE3) extract. rSpike was injected into two
602 immunization sections in 20 zebrafish females (previously anesthetized with tricaine
603 methanesulfonate (Sigma) - at a dose of 150 mg/L) at an interval of 7 days, with the aim
604 of producing plasma antibodies. Passive antibody transfer to zebrafish eggs occurs
605 naturally as described by Wang and collaborators²⁰. After immunization, females were
606 stimulated to mate (at 7 and 14 days after injection) and generated eggs. The time at

607 which the antibodies were transferred to the eggs was analyzed by the western blot
608 technique. Another control group was performed using 1 µg of a mix of proteins in
609 buffer 50 mM Tris-HCl pH 8.0, 200mM NaCl, and 1mM EDTA: equivalent amount of
610 purified PilZ protein from *Xanthomonas citri* (DOI: 10.1016/j.jmb.2009.07.065) and
611 LIC_11128 (residues 1-115 cloned into pET28a expression vector a with a fusion of
612 seven histidine tag at the N-terminal portion of the protein) from *Leptospira*
613 *interrogans*.

614

615 **Antibody responses in zebrafish**

616 Using SDS-PAGE protein electrophoresis, protein from fertilized eggs (10
617 µg/mL) and serum (10 µg/mL) from adult fish content (after 0, 7 and 14 days) were
618 assessed using methods described by Laemmli⁶⁸. The gels were subsequently stained
619 with 0.25% Coomassie brilliant blue R (Sigma-Aldrich, St. Louis, MO, USA).
620 Molecular weight and protein fraction levels were determined using readings from a
621 computerized densitometer in R software. To identify the protein content, different
622 markers for molecular weights were used and these ranged from 20 to 200 kDa. Protein
623 bands were excised from the SDS-polyacrylamide, and in-gel trypsin digestion was
624 performed according to Shevchenko et al.⁶⁹ and the identification by mass spectrometry.
625 Proteins were precipitated from plasma samples with 4 volumes of cold acetone and 1
626 volume of cold methanol. The in-solution trypsin digestion was performed according to
627 Lopes Ferreira and collaborators⁷⁰. Mass spectrometric analysis was done by LC-
628 MS/MS.

629

630 **Histology from multiple organs**

631 Fixation and decalcification of the adult zebrafish for histology and
632 immunofluorescence was performed according to Moore et al.⁷¹. For histopathological
633 analysis, 5-µm-thickness sections were mounted on slides and dewaxed in an oven at
634 60°C and hydrated in decreasing solutions of xylol three times, and once in xylol +
635 alcohol, for 10 minutes each, followed by a 100, 90, 80, and 70% alcohol battery and
636 washed with distilled water for five minutes. They were then stained with hematoxylin
637 and eosin for observation of the general cellular structures.

638

639 **Immunofluorescence assay and image acquisition**

640 For the immunofluorescence assays, the tissues from zebrafish were obtained 0,
641 7, and 14 days after intraperitoneal injection of SARS-CoV-2 viral protein. Zebrafish
642 tissue sections (5 μ m) mounted onto electrically charged slides to increase adherence
643 were deparaffinized in xylol. The samples underwent three 10-minute baths in xylol
644 (P.A.) and a final bath in ethanol/xylol solution (1:1) for 2 minutes. After being
645 deparaffinized, the samples were subjected to hydration by a sequence of ethanol baths
646 at decreasing concentrations (100%, 95%, 90%, 80%, 70%) for 2 minutes in each one,
647 followed by three washes in distilled water. Once hydrated, antigen retrieval was
648 performed by using a trypsin/phosphate-buffered solution (pH 7.2-7.3) mixture (1:1) at
649 37°C for 30 minutes in a laboratory drying oven (Thermo Fisher Scientific). Next, the
650 blockade of unspecific epitopes was achieved by a 60-minute incubation in a solution
651 comprised of 2% bovine serum albumin (Sigma Aldrich) (w/v), 0.3% Triton 100X
652 (v/v), and phosphate-buffered solution (pH 7.2-7.3). After that, the primary antibodies
653 were diluted in the aforementioned solution as follows: anti-Ly6G (1:300, Invitrogen,
654 Clone RB6-8C5, Cat 14-5931-81, host: rabbit), anti-AIF-1/Iba1 (1:300, Novus
655 Biologicals, Cat NB100-1028, host: goat) or (1:300, Abcam, Cat ab5076, host: goat),
656 anti-CD4/FITC-conjugated (1:200, eBioscience, Clone RM4-5, Cat 11-0042-85), and
657 anti-CD8/APC.Cy7-conjugated (1:200, BD Bioscience, Clone 53-6.7, Cat 557654). The
658 samples were incubated in these primary antibodies overnight at 4°C. Then, the samples
659 were washed three times in phosphate-buffered solution (pH 7.2-7.3) for 5 minutes
660 each. Secondary antibodies for anti-Ly6G and anti-Iba1 primary antibodies were
661 diluted as described above, as follows: anti-rabbit/Alexa488 (1:600, Invitrogen, Cat
662 A21206, host: donkey) and anti-goat/Alexa594 (1:600, Invitrogen, Cat A11058, host:
663 donkey). Incubation in these antibodies lasted 2 hours at room temperature. After
664 incubation, the samples were washed three times in phosphate-buffered solution (pH
665 7.2-7.3) for 10 minutes each. After the final wash, the samples were mounted with a
666 fluoromount containing DAPI dye (VectaShield). Finally, the slides were analyzed
667 under an Olympus VS120 microscope under 20x magnification to acquire images of the
668 whole zebrafish organism before focal analyses of the profile of the immune cells were
669 performed in specific zebrafish structures, which in turn was done by using an Axio

670 Observer combined with LSM 780 confocal device (Carl Zeiss) under the 630x
671 magnification lens.

672

673 **Bioinformatics *in silico* analysis**

674 **Annotation of ontological**

675 The zebrafish and human proteins related to the subcellular location (cytoplasm,
676 membrane, and nucleus) were recovered according to the annotation of ontological
677 terms in the ENSEMBL database (<https://www.ensembl.org/index.html>, accessed
678 06/04/2020). For each subcellular location, protein-protein interactions were predicted
679 with a SARS-CoV-2 Spike N-terminal fragment, residues 16-165, (rSpike) using the
680 UNISPPi predictor, where only interactions with a score greater than 0.95 were
681 accepted as interactions⁷². The interacted proteins were submitted to functional
682 enrichment to identify biological pathways using the G:Profiler software⁷³, based on the
683 database of zebrafish and human. In addition, the proteins were analyzed with the
684 Bioconductor Pathview package⁷⁴ in the R environment in search of the biological
685 pathways. The pathways were obtained from the Kyoto Encyclopedia of Genes and
686 Genomes (KEGG) database⁷⁵ and the model organism selected was the zebrafish and
687 human.

688

689 **Network analysis**

690 Samples were analyzed in triplicate, and their molecular masses and isoelectric
691 points of the proteins identified by MS / MS were observed using the ProtParam tool
692 (<http://us.expasy.org/tools/protparam.html>). Data normalization was performed, and a
693 significance cutoff was applied for the identified proteins at log-fold change ± 1.0 .
694 Subsequently, the identified proteins on the UniprotKB database were blasted against
695 zebrafish All data obtained were mapped using STRING web tool v11.0 ([https://string-
696 db.org/](https://string-db.org/)) to screen for protein-protein interactions (PPI).

697

698 ***In silico* analysis**

699 For *in silico* analysis, all FASTA sequences of proteins from zebrafish and
700 human, and SARS-CoV-2 were downloaded from the UNIPROT database
701 (<http://www.uniprot.org>). We then evaluated the subcellular localization of the
702 identified proteins using the CELLO (subcellular localization predictor) platform v.2.5
703 (<http://cello.life.nctu.edu.tw/>) and visualized the proteoform in the cleavage proteins in
704 Protter v. 1.0 (<http://wlab.ethz.ch/protter/start/>). In addition, the percentage of similarity
705 between the orthologous proteins of different species was calculated using the
706 EMBOSS Water platform (<https://www.ebi.ac.uk>), and protein alignments were
707 performed using the ESPript platform ([http://esprict.ibcp.fr/ESPript/cgi-](http://esprict.ibcp.fr/ESPript/cgi-bin/ESPript.cgi)
708 [bin/ESPript.cgi](http://esprict.ibcp.fr/ESPript/cgi-bin/ESPript.cgi)). For comparison of 3D structures, the FASTA files were converted into
709 PDB files (containing the 3D coordinates of the proteins) using the Raptor X tool
710 (<http://raptorx.uchicago.edu>). Then, structural similarities were compared on the iPDA
711 platform (<http://www.dsimb.inserm.fr>), and structural images of proteins were done
712 using the PyMOL software (<https://pymol.org/2/>). For the study of protein-protein
713 interaction and Docking of Spike peptides were performed using the Molsoft
714 MolBrower 3.9-1b software.

715

716

717

718

719

720

721

722

723

724

725

726 **Tables**

727 **Table 1. Summary of histopathological findings in different organs of zebrafish**
 728 **injected with rSpike.** Number of female fish with histopathological alterations out of
 729 total female fish injected. Females were injected either with Naïve control (n = 5),
 730 Control 1 (protein buffer) (n = 5), or SARS-CoV-2 protein (n =20).

System	Organs	Changes/Pathology	NAIV E	Control 1	SARS-CoV- 2 SPIKE
Circulatory	Heart	Lymphoid foci	0/5	0/5	1/20
	Kidney	Renal thrombosis	0/5	0/5	2/20
	Liver	Hyperemia	0/5	1/5	2/20
	Spleen	Hyperemia	0/5	0/5	0/20
Reproductive	Ovary	Atresic follicles	0/5	1/5	6/20
Nervous	Brain	Lymphoid foci	0/5	0/5	3/20
Digestive	Intestine	-	0/5	0/5	1/20
Urinary	Kidney	Presence of pigments, tubular and Bowman capsule structural integrity loss	0/5	0/5	2/20
Fotoreceptor	Eye	-	0/5	0/5	0/20
Endocrine	Langehans islands	-	0/5	0/5	0/20
Tegumentar		-	0/5	0/5	0/20
Respiratory	Gills	-	0/5	0/5	0/20

731

732

733

734

735







736

737

738

739

740 **Table 2.** Number of proteins identifying in each cellular component and in the protein-
 741 protein interaction prediction.

CC	N° of proteins	Total of interaction	SARS-CoV-2 interaction	Organism
Cytoplasm	3003	46757	771	
Cytoplasm	5677	76972	1168	
Membrane	7461	493258	2910	
Membrane	7779	161956	1785	
Nucleus	3887	84794	1134	
Nucleus	5501	78509	1242	

742

743 CC: cellular component; N° of proteins: the total number of proteins annotated to the
 744 specific subcellular component; total of interaction: the total number of interactions in
 745 the protein-protein interaction predicted and SARS-CoV-2 interaction: the number of
 746 protein interactions to the SARS-CoV-2 fragment in the protein-protein interaction
 747 prediction, Species: zebrafish and human.

748

749

750

751

752

753

754

755

756

757

758

759

760

761

762

763 **Figure legends**

764 **Figure 1. rSpike protein and its effects on the humoral immune response *in silico***
765 **and *in vivo* in zebrafish.** (a-a.1) Cryo-EM structure of the SARS-CoV-2 Spike Protein
766 (PDBID 6cs2.1, chain A) highlighting the residues 16-165 in blue (Pep1), in red (Pep2),
767 and yellow (Pep53). (a.2) Representation of the peptide 1 (residues 14-22), oxygen,
768 nitrogen and carbon are colored in red, blue and pink, respectively. (b) Free binding
769 energy of SARS-CoV-2 Spike Pep1, Pep 2, and Pep 3 in complex with MHC II, MHC I,
770 TCR alpha, and TCR beta of human (grey dots) and zebrafish (blue dots) based on
771 docking analysis and the axis (X) represents the score of 10 (ten) possibilities of
772 interaction between molecule-ligand and the axis (Y) compares the free binding energy
773 it represents per kilocalorie per mol (Kcal/mol). (c) Comparison of topological location
774 and insertion of Pep 1 in the receptor protein binding site from zebrafish (bottom panel)
775 and human (top panel) MHC II, MHC I, TCR alpha, and TCR beta. The amino acid
776 receptor residues are shown on the protein surface in orange colors; red and blue
777 represented by the chemical elements. (d) Structural alignment of the IgM
778 constant/heavy chain between zebrafish and human. (e) Densitometry of 100 kDa bands
779 from adult female serum separated by a SDS-PAGE (red colored box): M: molecular
780 weight marker (company) and the red dotted box correspond to intensities of the bands
781 from the SDS-PAGE of naïve female serum (box 1), IgM production from immunized
782 zebrafish with buffer (box 2), and rSpike protein (residues 16-165) after 7 (box 3) and
783 14 (box 4) days. (f) Densitometry of 100 kDa bands of a SDS-PAGE gel loaded with
784 eggs extract from naïve (1) and female injected with rSpike (residues 16-165) after 7 (2)
785 and 14 days (3). (g, h) Graphs representation of densitometry quantification of serum
786 (g) and egg (h) IgM levels showed in panel e and panel f, respectively, demonstrating an
787 increase of IgM production by immunized females (red bars). Control naïve are fishes
788 not treated, Control 1 are fishes treated with buffer and rSpike protein (spike residues
789 16-165).

790 **Figure 2. rSpike protein injection is toxic to adult female zebrafish.** Graph of
791 survival rate and days after immunization. Kaplan-Meier cumulative probability curve
792 indicating survival rate of zebrafish after two immunization with different protein
793 samples. Females were injected either with rSpike protein, extract of lysed *E.coli* cells,
794 buffer presented the rSpike protein (control 1), naïve control (not immunized), or a mix
795 of two recombinant protein: PilZ protein from *Xanthomonas citri* and N-terminal part of

796 LIC_11128 from *Leptospira interrogans* Copenhageni (control 2). Each group was
797 performed using adult female fishes.

798

799 **Figure 3. Inflammatory infiltrates in different systems of zebrafish injected with**
800 **rSpike protein. a:** longitudinal section of the whole female zebrafish for morphological
801 analyses of the main organs affected. All sections were stained with Hematoxylin Eosin.
802 **Brain:** (b)- histology of control, (c)- brain histology after 7 days of first immunization
803 presenting macrophages, and (d) 14 days after first immunization with a burst after 7
804 days from the first immunization presenting intense mononuclear infiltrate. (e) The
805 same image as panel d but at a higher magnification. **Ovary:** Ovarian histology from
806 zebrafish control (f), after 7 (g - h) and 14 days (i). (f-i) Follicular development was
807 classified as primary growth oocyte (PG), cortical alveolus (CA), and vitellogenic (V)
808 stages. Asterisks in panel g indicate an abundant and disorganized extracellular matrix
809 in the ovarian stroma. (h) Inset shows a higher magnification of the cellular infiltration
810 and arrows show dense, eosinophilic inflammatory infiltrates. (i) The histology of
811 ovaries after 14 days is similar to the control. Scale bars: 1000 μm (g) and 200 μm (f, h,
812 and i). **Liver:** Histology of the liver from control (j), after 7 days from rSpike
813 immunization (l), and after 14 days from the first immunization with a burst at 7 days
814 (m). **Kidney:** Histology of kidney from zebrafish control (n), after 7 days from the first
815 immunization (o), and after 14 days from the first immunization with a second
816 immunization after 7 days (p). Scale bars: 1,000 μm (n) and 200 μm (o - p).

817

818 **Figure 4. rSpike protein immunization induces systemic neutrophil and**
819 **macrophage infiltration in zebrafish.** Representative immunofluorescence from
820 zebrafish non-immunized control (a) and i.p. immunized with rSpike protein 7 days
821 post-immunization and assessed by scan scope (b). Overview of the whole fish (a1-a5,
822 b1-b4). (c) Confocal-multiphoton imaging from zebrafish immunized twice with rSpike
823 protein after 14 days from the first immunization. The second immunization happened 7
824 days after the first one. The images depict DAPI (nucleic acid colored in blue), Ly6G
825 (neutrophils colored in green), and Iba1 (macrophages colored in red). Colocalization of
826 DAPI, Ly6G, and Iba1 between fishes are shown in panels described as Overlay. The

827 assay was performed using 7 adult female fishes for immunized groups and adult female
828 fishes for non-immunized group, used as a control group.

829

830 **Figure 5. rSpike protein immunization induces innate immune system responses in**
831 **zebrafish.** Immunofluorescence from zebrafish i.p. immunized with rSpike protein after
832 7 (a-d) and 14 (e-h) days of injection. The images depict DAPI (nucleic acid colored in
833 blue), CD4 (colored in green), and CD8 (colored in red). Colocalization of DAPI, CD4,
834 and CD8 between fish injected are shown in panels d and h (described as Overlay). The
835 assay was performed using 7 adult female fishes for immunized groups.

836

837 **Figure 6. *In silico* analysis of the interaction of the human and zebrafish ACE2**
838 **receptor with rSpike protein.** (a) Structural alignment between ACE2 of human and
839 zebrafish. For comparison of 3D structures, the FASTA files were converted into PDB
840 files (containing the 3D coordinates of the proteins) using the Raptor X tool
841 (<http://raptorx.uchicago.edu>). (b) The similarity of ACE2 between human and zebrafish.
842 (c) Graphs show the free binding energy in protein-ligand interactions docking analysis
843 and the axis (X) represents the score of 10 (ten) possibilities of interaction between
844 molecule-ligand and the axis (Y) compares the free binding energy it represents per
845 kilocalorie per mol (Kcal/mol). (Kcal/mol). (d) Protein-protein interaction between
846 human and zebrafish ACE2 and SARS-CoV-2 Spike RBD.

847

848 **Figure 7. Biological pathways enriched with proteins found from protein-protein**
849 **interaction prediction with rSpike.** Graph relating the proteins from zebrafish (a) and
850 human (b) predicted to interact to rSpike with its cell localization and function within
851 the cell (pathways).

852

853 **Figure 8. Schematic representation of the Toll-like receptor pathway and cytokine-**
854 **cytokine receptor interaction.** Biological pathway recovered through functional
855 enrichment and mapping of proteins interacting with the recombinant spike protein,
856 rSpike. In red (N) are proteins located in nucleus; dark orange (NM) shows proteins
857 identified in the nucleus and membrane; light orange (NC) shows proteins identified in
858 the nucleus and cytoplasm; yellow (CMN) shows proteins identified in the cytoplasm,
859 membrane, and nucleus; yellow-greenish (M) shows proteins identified in the
860 membrane; dark blue (CM) shows proteins identified in the cytoplasm and membrane;

861 and blue (C) shows proteins identified in the cytoplasm. The schematic represents the
862 zebrafish pathway (a) and the right side of the schematic represents the human pathway
863 (b). The functional enrichment of the pathways was performed with Gprofiler software,
864 and the mapping was performed with the Bioconductor Pathview package. Pathways
865 adapted from KEGG.

866

867 **Figure 9.** (a and b) Protein interaction network in zebrafish blood plasma. The strongest
868 interactions are exemplified by thicker lines and the weakest are shown by dotted lines.
869 (b) The proteins in red belong to the blood coagulation cascade and also to the immune
870 system pathway. The green proteins are those involved in the structural and
871 chromosome components. The STRING software was used to analyze the protein
872 network and Kyoto Encyclopedia at Genes and Genomes (KEGG) tool to detect
873 protein-protein association. Pvalb4, Parvalbumin 4; Ckma, Creatine kinase; Krt5,
874 Keratin 5; Ak1, A kinase (PRKA) anchor protein 1; Mdh1aa, Malate dehydrogenase; 24
875 Eno3, 2-phospho-D-glycerate hydro-lyase; ENSDARG00000095050, Component
876 Chromosome 15; wu:fk65c09, Component Chromosome 1; Zgc:114037, Component
877 Chromosome 16; Zgc:114046, Component Chromosome 17; ENSDARG00000088889,
878 Component Chromosome 26; Apoa2, Apolipoprotein A-II; Apo1b, Apolipoprotein A-
879 Ib; Serpina7, Serpin peptidase inhibitor, clade A (alpha-1 antiproteinase, antitrypsin),
880 member 7; Tmprss2, Transmembrane serine protease 2; Fetub, Fetuin B; Apo1a,
881 Apolipoprotein A-I; Ces3, Carboxylic ester hydrolase; Apobb, Apolipoprotein Bb,
882 tandem duplicate 1; Fga, Fibrinopeptide A; Tfa, Serotransferrin; Apoc1, Apolipoprotein
883 C-I; C9, Complement component C9; Crp, Pentaxin; Cp, Ceruloplasmin; Hpx,
884 Hemopexin; Ba1, Ba1 protein; ENSDARG00000, Component Chromosome 13; and
885 ENSDARG0000008912, Component Chromosome 25.

886

887 **Figure 10. Purification of rSipke protein.** a: 15% SDS-PAGE of rSpike purified
888 protein (lanes 1-3) after elution of the protein from exclusion chromatograph column.
889 Ma. Pierce™ Unstained Protein MW Marker (ThermoFisher scientific). b: Western
890 blotting to detect polyhistidine proteins. The protein molecular weight marker (Ma), a
891 not induced *E. coli* BL21(DE3) cells (1) containing the pET28a vector to express rSpike
892 and purified rSpike protein (2) were loaded to a 15% SDS-PAGE and transferred to a
893 nitrocellulose membrane. The membrane was initially blocked with 5% skin milk with

894 PBS buffer for 2 hours and after few PBS rinse the membrane was incubated with
895 monoclonal Anti-polyHistidine–Peroxidase antibody produced in mouse (Sigma-
896 Aldrich).

897

898 **Bibliography**

- 899 1. Peiris M, Leung GM. What can we expect from first-generation COVID-19
900 vaccines? *Lancet*. September 2020. doi:10.1016/S0140-6736(20)31976-0
- 901 2. Rajan B, Løkka G, Koppang EO, Austbø L. Passive Immunization of Farmed
902 Fish. *J Immunol*. 2017;198(11):4195-4202. doi:10.4049/jimmunol.1700154
- 903 3. Berghmans S, Jette C, Langenau D, et al. Making waves in cancer research: new
904 models in the zebrafish. *Biotechniques*. 2005;39(2):227-237.
905 doi:10.2144/05392RV02
- 906 4. Howe K, Clark MD, Torroja CF, et al. The zebrafish reference genome sequence
907 and its relationship to the human genome. *Nature*. 2013;496(7446):498-503.
908 doi:10.1038/nature12111
- 909 5. Bailone RL, Fukushima HCS, Ventura Fernandes BH, et al. Zebrafish as an
910 alternative animal model in human and animal vaccination research. *Lab Anim*
911 *Res*. 2020;36(1):13. doi:10.1186/s42826-020-00042-4
- 912 6. Charlie-Silva I, Feitosa NM, Gomes JMM, et al. Potential of mucoadhesive
913 nanocapsules in drug release and toxicology in zebrafish. Mukherjee A, ed. *PLoS*
914 *One*. 2020;15(9):e0238823. doi:10.1371/journal.pone.0238823
- 915 7. MacRae CA, Peterson RT. Zebrafish as tools for drug discovery. *Nat Rev Drug*
916 *Discov*. 2015;14(10):721-731. doi:10.1038/nrd4627
- 917 8. Lurie N, Saville M, Hatchett R, Halton J. Developing Covid-19 Vaccines at
918 Pandemic Speed. *N Engl J Med*. 2020;382(21):1969-1973.
919 doi:10.1056/NEJMp2005630
- 920 9. Singh A, Singh RS, Sarma P, et al. A Comprehensive Review of Animal Models
921 for Coronaviruses: SARS-CoV-2, SARS-CoV, and MERS-CoV. *Virol Sin*.

- 922 2020;35(3):290-304. doi:10.1007/s12250-020-00252-z
- 923 10. Lu S, Zhao Y, Yu W, Yang Y, Gao J, Wang J. Comparison of SARS-CoV-2
924 infections among 3 species of non-human Affiliations : :1-27.
- 925 11. Niu J, Shen L, Huang B, et al. Non-invasive bioluminescence imaging of HCoV-
926 OC43 infection and therapy in the central nervous system of live mice. *Antiviral*
927 *Res.* 2020;173:104646. doi:10.1016/j.antiviral.2019.104646
- 928 12. Hanke L, Vidakovics Perez L, Sheward DJ, et al. An alpaca nanobody neutralizes
929 SARS-CoV-2 by blocking receptor interaction. *Nat Commun.* 2020;11(1):1-9.
930 doi:10.1038/s41467-020-18174-5
- 931 13. Cunha LE, Stolet A, Strauch M, et al. Equine hyperimmune globulin raised
932 against the SARS-CoV-2 spike glycoprotein has extremely high neutralizing
933 titers. 2020:1-28. doi:<https://doi.org/10.1101/2020.08.17.254375> .
- 934 14. Zylberman V, Sanguineti S, Pontoriero A V, et al. Development of a
935 hyperimmune equine serum therapy for COVID-19 in Argentina. *Medicina (B*
936 *Aires)*. 2020;80 Suppl 3:1-6. <http://www.ncbi.nlm.nih.gov/pubmed/32658841>.
- 937 15. Deng J, Jin Y, Liu Y, et al. Serological survey of SARS-CoV-2 for experimental,
938 domestic, companion and wild animals excludes intermediate hosts of 35
939 different species of animals. *Transbound Emerg Dis.* 2020;67(4):1745-1749.
940 doi:10.1111/tbed.13577
- 941 16. Galindo-Villegas J. The Zebrafish Disease and Drug Screening Model: A Strong
942 Ally Against Covid-19. *Front Pharmacol.* 2020;11.
943 doi:10.3389/fphar.2020.00680
- 944 17. Gaudin R, Goetz JG. Tracking Mechanisms of Viral Dissemination In Vivo.
945 *Trends Cell Biol.* October 2020. doi:10.1016/j.tcb.2020.09.005
- 946 18. Sawicki SG, Sawicki DL, Siddell SG. A Contemporary View of Coronavirus
947 Transcription. *J Virol.* 2007;81(1):20-29. doi:10.1128/JVI.01358-06
- 948 19. Long QX, Liu BZ, Deng HJ, et al. Antibody responses to SARS-CoV-2 in
949 patients with COVID-19. *Nat Med.* 2020;26(6):845-848. doi:10.1038/s41591-

- 950 020-0897-1
- 951 20. Wang H, Ji D, Shao J, Zhang S. Maternal transfer and protective role of
952 antibodies in zebrafish *Danio rerio*. *Mol Immunol*. 2012;51(3-4):332-336.
953 doi:10.1016/j.molimm.2012.04.003
- 954 21. Swain P, Nayak SK. Role of maternally derived immunity in fish. *Fish Shellfish*
955 *Immunol*. 2009;27(2):89-99. doi:10.1016/j.fsi.2009.04.008
- 956 22. Yu Y, Xu J, Li Y, Hu Y, Li B. Breast Milk-fed Infant of COVID-
957 19 Pneumonia Mother: a Case Report. 2020:1-11. doi:10.21203/rs.3.rs-
958 20792/v1
- 959 23. Demers-Mathieu V, Dung M, Mathijssen GB, et al. Difference in levels of
960 SARS-CoV-2 S1 and S2 subunits- and nucleocapsid protein-reactive SIgM/IgM,
961 IgG and SIgA/IgA antibodies in human milk. *J Perinatol*. September 2020.
962 doi:10.1038/s41372-020-00805-w
- 963 24. Munz M, Wessendorf S, Koretsis G, et al. Acute transverse myelitis after
964 COVID-19 pneumonia. *J Neurol*. 2020;267(8):2196-2197. doi:10.1007/s00415-
965 020-09934-w
- 966 25. Xu Z, Shi L, Wang Y, et al. Pathological findings of COVID-19 associated with
967 acute respiratory distress syndrome. *Lancet Respir Med*. 2020;8(4):420-422.
968 doi:10.1016/S2213-2600(20)30076-X
- 969 26. Lu Y, Li X, Geng D, et al. Cerebral Micro-Structural Changes in COVID-19
970 Patients – An MRI-based 3-month Follow-up Study. *EClinicalMedicine*.
971 2020;25:100484. doi:10.1016/j.eclinm.2020.100484
- 972 27. Cavalcanti DD, Raz E, Shapiro M, et al. Cerebral Venous Thrombosis Associated
973 with COVID-19. *Am J Neuroradiol*. 2020;41(8):1370-1376.
974 doi:10.3174/ajnr.A6644
- 975 28. Iadecola C, Anrather J, Kamel H. Effects of COVID-19 on the Nervous System.
976 *Cell*. August 2020. doi:10.1016/j.cell.2020.08.028
- 977 29. Lau K-K, Yu W-C, Chu C-M, Lau S-T, Sheng B, Yuen K-Y. Possible Central

- 978 Nervous System Infection by SARS Coronavirus. *Emerg Infect Dis.*
979 2004;10(2):342-344. doi:10.3201/eid1002.030638
- 980 30. Netland J, Meyerholz DK, Moore S, Cassell M, Perlman S. Severe Acute
981 Respiratory Syndrome Coronavirus Infection Causes Neuronal Death in the
982 Absence of Encephalitis in Mice Transgenic for Human ACE2. *J Virol.*
983 2008;82(15):7264-7275. doi:10.1128/JVI.00737-08
- 984 31. Tian S, Xiong Y, Liu H, et al. Pathological study of the 2019 novel coronavirus
985 disease (COVID-19) through postmortem core biopsies. *Mod Pathol.*
986 2020;33(6):1007-1014. doi:10.1038/s41379-020-0536-x
- 987 32. Beghi E, Feigin V, Caso V, Santalucia P, Logroscino G. COVID-19 Infection
988 and Neurological Complications: Present Findings and Future Predictions.
989 *Neuroepidemiology.* July 2020:1-6. doi:10.1159/000508991
- 990 33. Sotoca J, Rodríguez-Álvarez Y. COVID-19-associated acute necrotizing
991 myelitis. *Neurol - Neuroimmunol Neuroinflammation.* 2020;7(5):e803.
992 doi:10.1212/NXI.0000000000000803
- 993 34. Wright EJ, Brew BJ, Wesselingh SL. Pathogenesis and Diagnosis of Viral
994 Infections of the Nervous System. *Neurol Clin.* 2008;26(3):617-633.
995 doi:10.1016/j.ncl.2008.03.006
- 996 35. Abdel-Mannan O, Eyre M, Löbel U, et al. Neurologic and Radiographic Findings
997 Associated With COVID-19 Infection in Children. *JAMA Neurol.* July 2020.
998 doi:10.1001/jamaneurol.2020.2687
- 999 36. Campochiaro C, Dagna L. The conundrum of interleukin-6 blockade in COVID-
1000 19. *Lancet Rheumatol.* 2020;2(10):e579-e580. doi:10.1016/S2665-
1001 9913(20)30287-3
- 1002 37. Sinha P, Mostaghim A, Bielick CG, et al. Early administration of interleukin-6
1003 inhibitors for patients with severe COVID-19 disease is associated with
1004 decreased intubation, reduced mortality, and increased discharge. *Int J Infect Dis.*
1005 2020;99:28-33. doi:10.1016/j.ijid.2020.07.023

- 1006 38. Casanova J-L, Holland SM, Notarangelo LD. Inborn Errors of Human JAKs and
1007 STATs. *Immunity*. 2012;36(4):515-528. doi:10.1016/j.immuni.2012.03.016
- 1008 39. Baris S, Alroqi F, Kiykim A, et al. Severe Early-Onset Combined
1009 Immunodeficiency due to Heterozygous Gain-of-Function Mutations in STAT1.
1010 *J Clin Immunol*. 2016;36(7):641-648. doi:10.1007/s10875-016-0312-3
- 1011 40. Goswami R, Kaplan MH. STAT Transcription Factors in T Cell Control of
1012 Health and Disease. In: ; 2017:123-180. doi:10.1016/bs.ircmb.2016.09.012
- 1013 41. Sugawara I, Yamada H, Mizuno S. STAT1 Knockout Mice are Highly
1014 Susceptible to Pulmonary Mycobacterial Infection. *Tohoku J Exp Med*.
1015 2004;202(1):41-50. doi:10.1620/tjem.202.41
- 1016 42. Guo Y, Pan W, Liu S, Shen Z, Xu Y, Hu L. ERK/MAPK signalling pathway and
1017 tumorigenesis (Review). *Exp Ther Med*. January 2020.
1018 doi:10.3892/etm.2020.8454
- 1019 43. Janka GE, Lehmborg K. Hemophagocytic syndromes — An update. *Blood Rev*.
1020 2014;28(4):135-142. doi:10.1016/j.blre.2014.03.002
- 1021 44. Kudose S, Batal I, Santoriello D, et al. Kidney Biopsy Findings in Patients with
1022 COVID-19. *J Am Soc Nephrol*. 2020;31(9):1959-1968.
1023 doi:10.1681/ASN.2020060802
- 1024 45. Pan X, Xu D, Zhang H, Zhou W, Wang L, Cui X. Identification of a potential
1025 mechanism of acute kidney injury during the COVID-19 outbreak: a study based
1026 on single-cell transcriptome analysis. *Intensive Care Med*. 2020;46(6):1114-
1027 1116. doi:10.1007/s00134-020-06026-1
- 1028 46. Ronco C, Reis T. Kidney involvement in COVID-19 and rationale for
1029 extracorporeal therapies. *Nat Rev Nephrol*. 2020;16(6):308-310.
1030 doi:10.1038/s41581-020-0284-7
- 1031 47. Deng Y, Liu W, Liu K, et al. Clinical characteristics of fatal and recovered cases
1032 of coronavirus disease 2019 in Wuhan, China: a retrospective study. *Chin Med J*
1033 (*Engl*). 2020;133(11):1261-1267. doi:10.1097/CM9.0000000000000824

- 1034 48. Cai Q, Huang D, Yu H, et al. COVID-19: Abnormal liver function tests. *J*
1035 *Hepatol.* 2020;73(3):566-574. doi:10.1016/j.jhep.2020.04.006
- 1036 49. Agius C, Roberts RJ. Melano-macrophage centres and their role in fish
1037 pathology. *J Fish Dis.* 2003;26(9):499-509. doi:10.1046/j.1365-
1038 2761.2003.00485.x
- 1039 50. Jothimani D, Venugopal R, Abedin MF, Kalamoorthy I, Rela M. COVID-19 and
1040 the liver. *J Hepatol.* June 2020. doi:10.1016/j.jhep.2020.06.006
- 1041 51. Reis FM, Bouissou DR, Pereira VM, Camargos AF, dos Reis AM, Santos RA.
1042 Angiotensin-(1-7), its receptor Mas, and the angiotensin-converting enzyme type
1043 2 are expressed in the human ovary. *Fertil Steril.* 2011;95(1):176-181.
1044 doi:10.1016/j.fertnstert.2010.06.060
- 1045 52. Vaz-Silva J, Carneiro MM, Ferreira MC, et al. The Vasoactive Peptide
1046 Angiotensin-(1—7), Its Receptor Mas and the Angiotensin-converting Enzyme
1047 Type 2 are Expressed in the Human Endometrium. *Reprod Sci.* 2009;16(3):247-
1048 256. doi:10.1177/1933719108327593
- 1049 53. Zupin L, Pascolo L, Zito G, Ricci G, Crovella S. SARS-CoV-2 and the next
1050 generations: which impact on reproductive tissues? *J Assist Reprod Genet.*
1051 August 2020. doi:10.1007/s10815-020-01917-0
- 1052 54. Jiang R-D, Liu M-Q, Chen Y, et al. Pathogenesis of SARS-CoV-2 in Transgenic
1053 Mice Expressing Human Angiotensin-Converting Enzyme 2. *Cell.*
1054 2020;182(1):50-58.e8. doi:10.1016/j.cell.2020.05.027
- 1055 55. Qiu Y, Zhao Y-B, Wang Q, et al. Predicting the angiotensin converting enzyme 2
1056 (ACE2) utilizing capability as the receptor of SARS-CoV-2. *Microbes Infect.*
1057 2020;22(4-5):221-225. doi:10.1016/j.micinf.2020.03.003
- 1058 56. Chou CF, Loh CB, Foo YK, et al. ACE2 orthologues in non-mammalian
1059 vertebrates (Danio, Gallus, Fugu, Tetraodon and Xenopus). *Gene.* 2006;377(1-
1060 2):46-55. doi:10.1016/j.gene.2006.03.010
- 1061 57. Bhattacharya M, Sharma AR, Patra P, et al. Development of epitope-based

- 1062 peptide vaccine against novel coronavirus 2019 (SARS-COV-2):
1063 Immunoinformatics approach. *J Med Virol.* 2020;92(6):618-631.
1064 doi:10.1002/jmv.25736
- 1065 58. Sunyer JO. Fishing for mammalian paradigms in the teleost immune system. *Nat*
1066 *Immunol.* 2013;14(4):320-326. doi:10.1038/ni.2549
- 1067 59. Flajnik MF. A cold-blooded view of adaptive immunity. *Nat Rev Immunol.*
1068 2018;18(7):438-453. doi:10.1038/s41577-018-0003-9
- 1069 60. Litman GW, Cannon JP, Dishaw LJ. Reconstructing immune phylogeny: new
1070 perspectives. *Nat Rev Immunol.* 2005;5(11):866-879. doi:10.1038/nri1712
- 1071 61. Mashoof S, Criscitiello M. Fish Immunoglobulins. *Biology (Basel).* 2016;5(4):45.
1072 doi:10.3390/biology5040045
- 1073 62. Rumfelt LL, Lohr RL, Dooley H, Flajnik MF. Diversity and repertoire of IgW
1074 and IgM VH families in the newborn nurse shark. *BMC Immunol.* 2004;5:1-15.
1075 doi:10.1186/1471-2172-5-8
- 1076 63. Hu Y-L, Xiang L-X, Shao J-Z. Identification and characterization of a novel
1077 immunoglobulin Z isotype in zebrafish: Implications for a distinct B cell receptor
1078 in lower vertebrates. *Mol Immunol.* 2010;47(4):738-746.
1079 doi:10.1016/j.molimm.2009.10.010
- 1080 64. Marianes AE, Zimmerman AM. Targets of somatic hypermutation within
1081 immunoglobulin light chain genes in zebrafish. *Immunology.* 2011;132(2):240-
1082 255. doi:10.1111/j.1365-2567.2010.03358.x
- 1083 65. Lewis KL, Del Cid N, Traver D. Perspectives on antigen presenting cells in
1084 zebrafish. *Dev Comp Immunol.* 2014;46(1):63-73. doi:10.1016/j.dci.2014.03.010
- 1085 66. Muñoz-Fontela C, Dowling WE, Funnell SGP, et al. Animal models for COVID-
1086 19. *Nature.* 2020. doi:10.1038/s41586-020-2787-6
- 1087 67. Tsang B, Zahid H, Ansari R, Lee RC-Y, Partap A, Gerlai R. Breeding Zebrafish:
1088 A Review of Different Methods and a Discussion on Standardization. *Zebrafish.*
1089 2017;14(6):561-573. doi:10.1089/zeb.2017.1477

- 1090 68. Laemmli UK. 227680a0. *Nature*. 1970;227:680-685.
- 1091 69. Shevchenko G, Konzer A, Musunuri S, Bergquist J. Neuroproteomics tools in
1092 clinical practice. *Biochim Biophys Acta - Proteins Proteomics*.
1093 2015;1854(7):705-717. doi:10.1016/j.bbapap.2015.01.016
- 1094 70. Babaei E, Alilu S, Laali S. A New General Topology for Cascaded Multilevel
1095 Inverters With Reduced Number of Components Based on Developed H-Bridge.
1096 *IEEE Trans Ind Electron*. 2014;61(8):3932-3939. doi:10.1109/TIE.2013.2286561
- 1097 71. Moore JL, Aros M, Steudel KG, Cheng KC. Fixation and Decalcification of
1098 Adult Zebrafish for Histological, Immunocytochemical, and Genotypic Analysis.
1099 *Biotechniques*. 2002;32(2):296-298. doi:10.2144/02322st03
- 1100 72. Valente GT, Acencio ML, Martins C, Lemke N. The Development of a Universal
1101 In Silico Predictor of Protein-Protein Interactions. Csermely P, ed. *PLoS One*.
1102 2013;8(5):e65587. doi:10.1371/journal.pone.0065587
- 1103 73. Reimand J, Arak T, Adler P, et al. g:Profiler—a web server for functional
1104 interpretation of gene lists (2016 update). *Nucleic Acids Res*. 2016;44(W1):W83-
1105 W89. doi:10.1093/nar/gkw199
- 1106 74. Luo W, Brouwer C. Pathview: an R/Bioconductor package for pathway-based
1107 data integration and visualization. *Bioinformatics*. 2013;29(14):1830-1831.
1108 doi:10.1093/bioinformatics/btt285
- 1109 75. Ogata H, Goto S, Sato K, Fujibuchi W, Bono H, Kanehisa M. KEGG: Kyoto
1110 Encyclopedia of Genes and Genomes. *Nucleic Acids Res*. 1999;27(1):29-34.
1111 doi:10.1093/nar/27.1.29

1112

1113

1114

1115

Figures

Figure 1

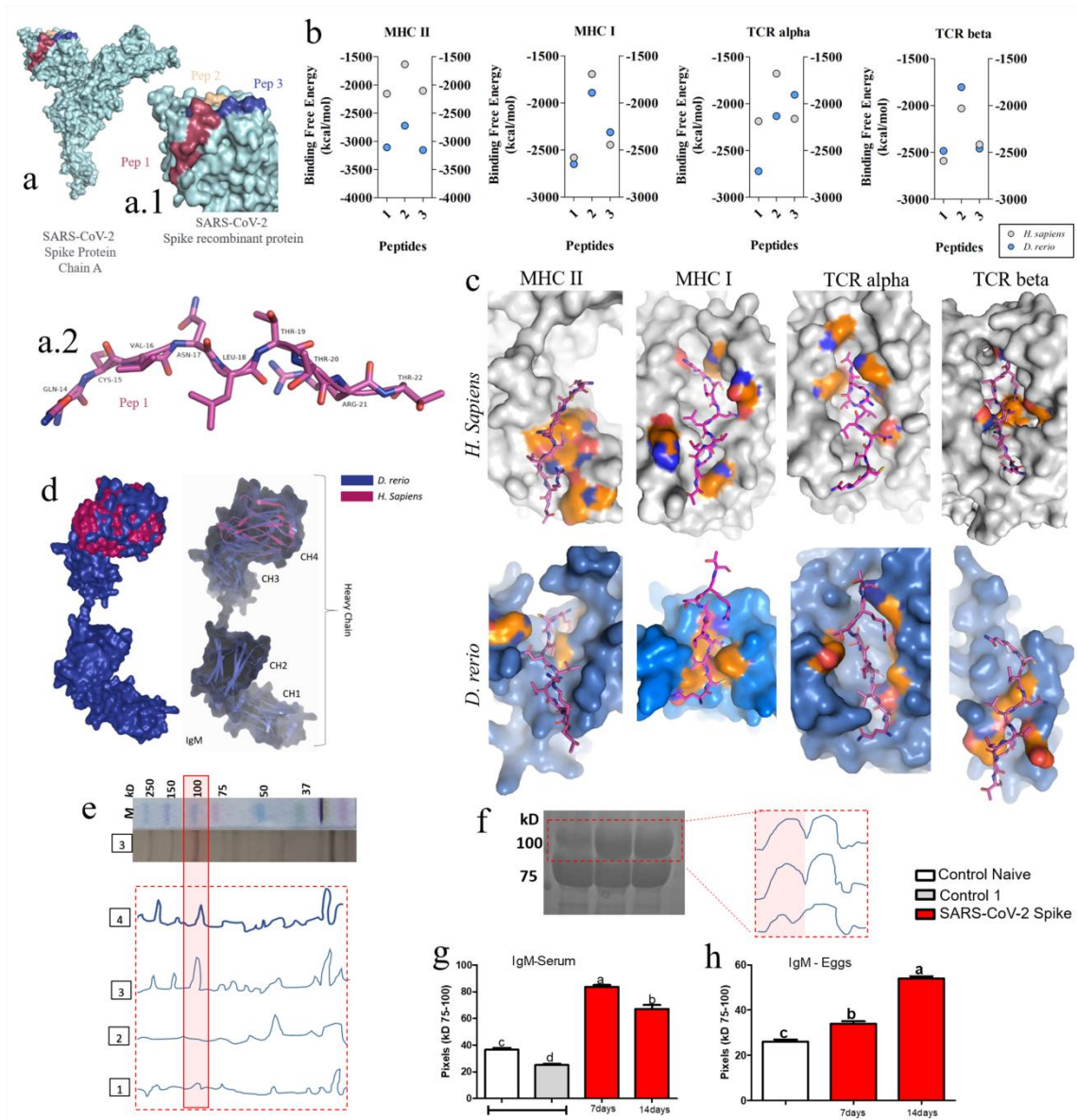


Figure 2

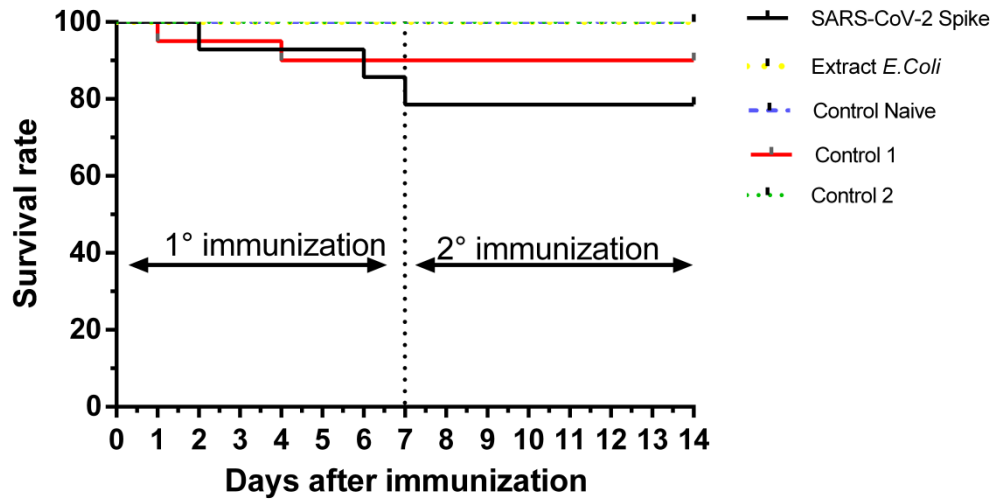


Figure 3

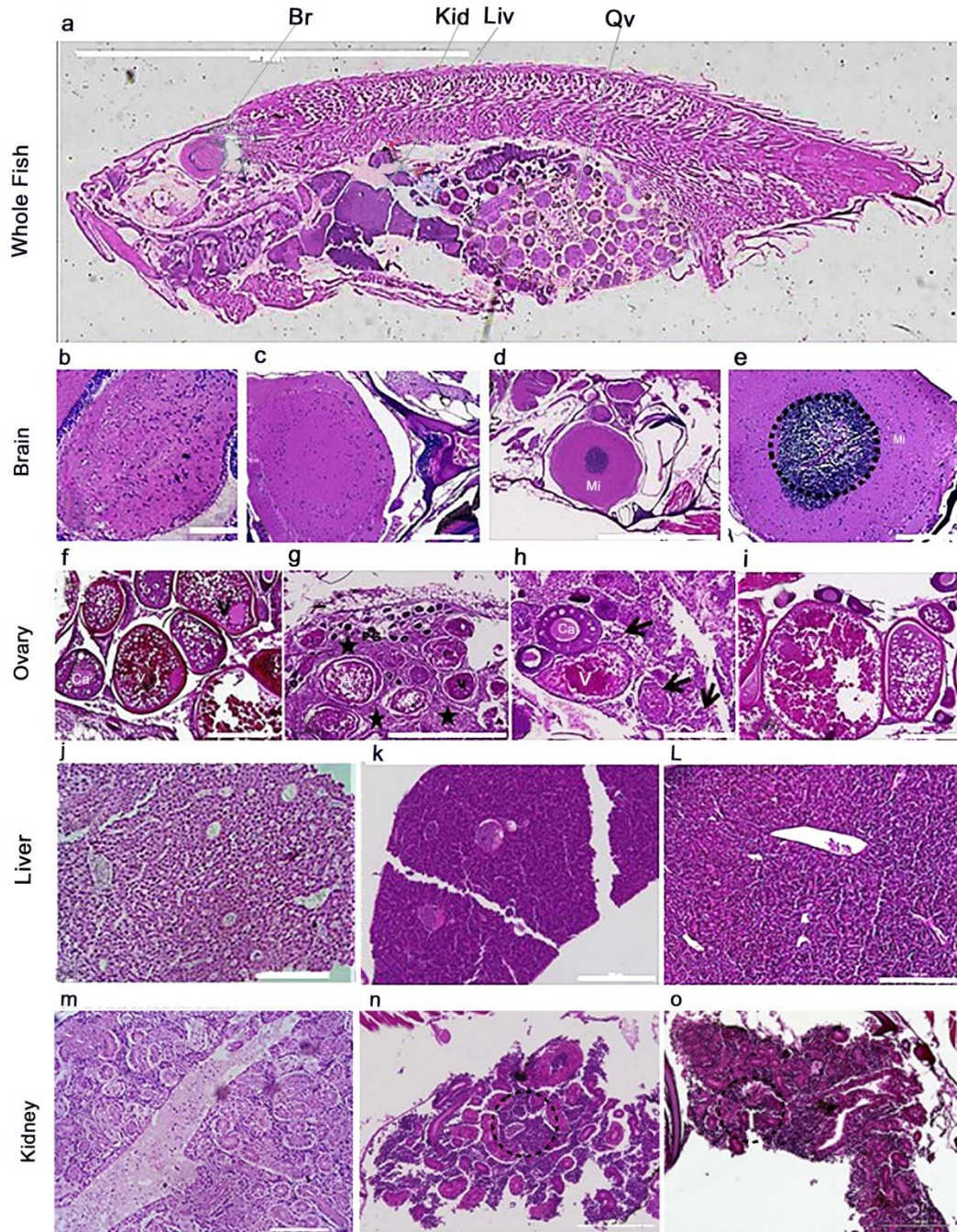
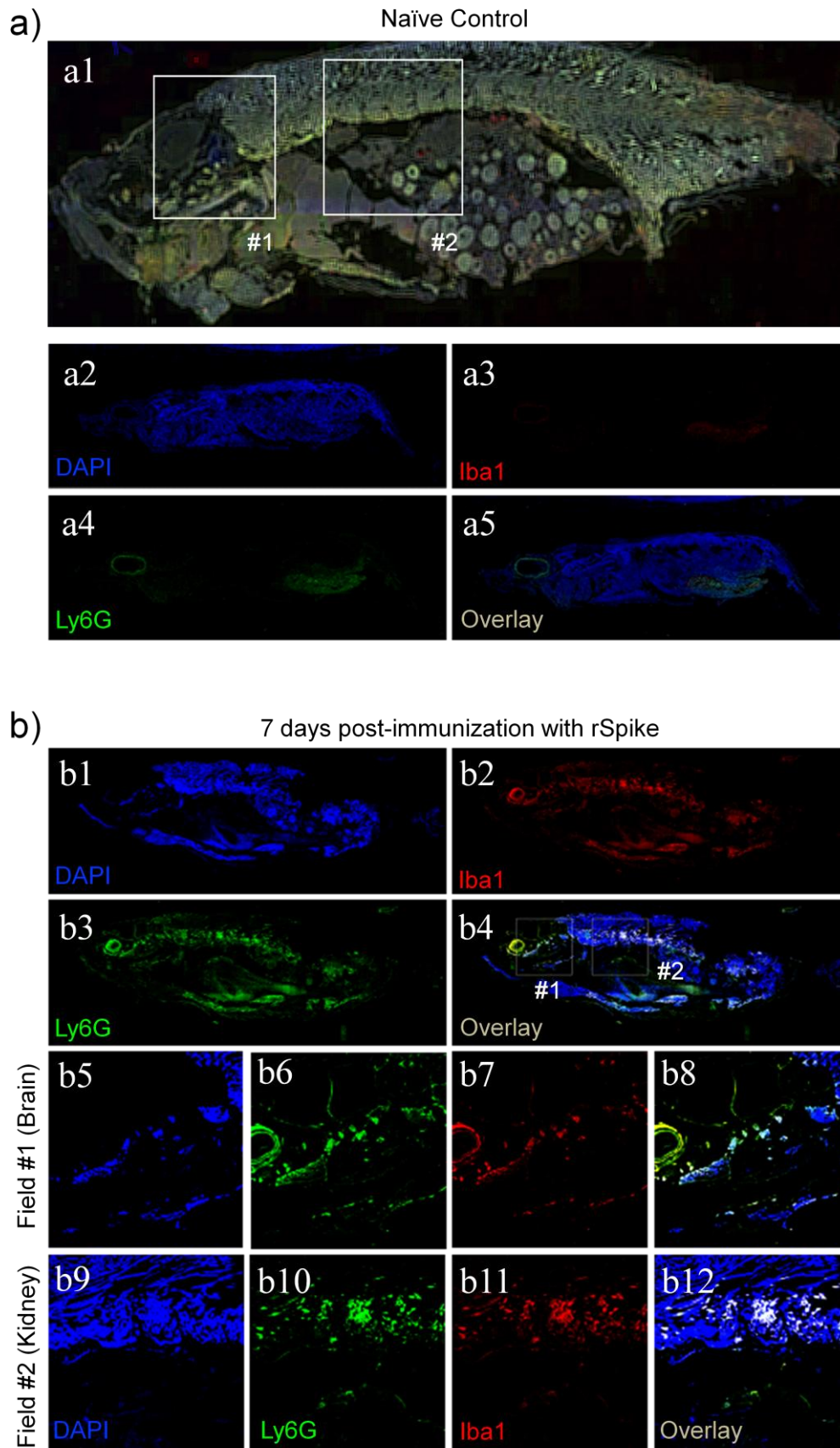


Figure 4



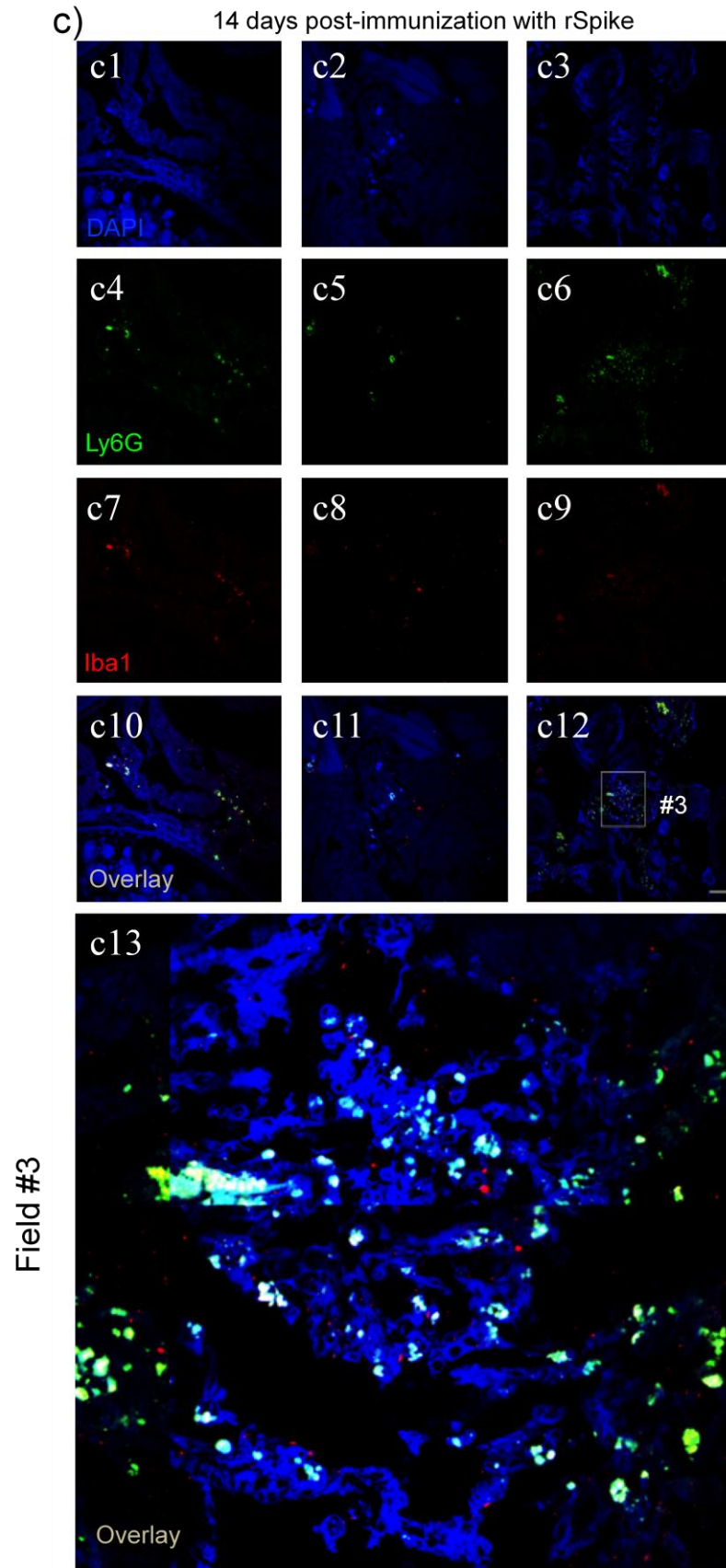


Figure 5

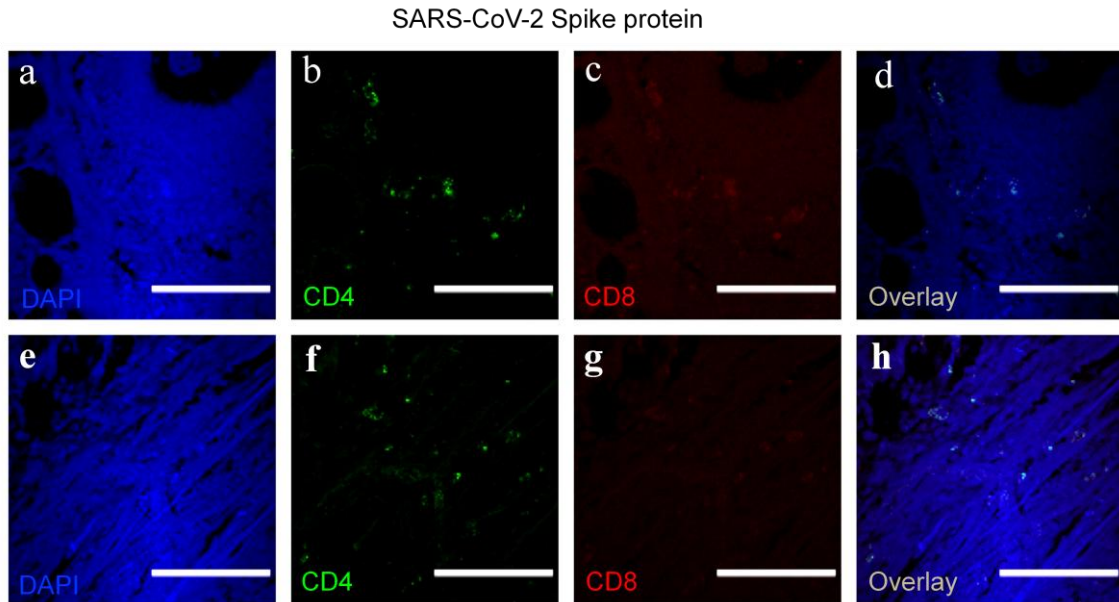


Figure 6

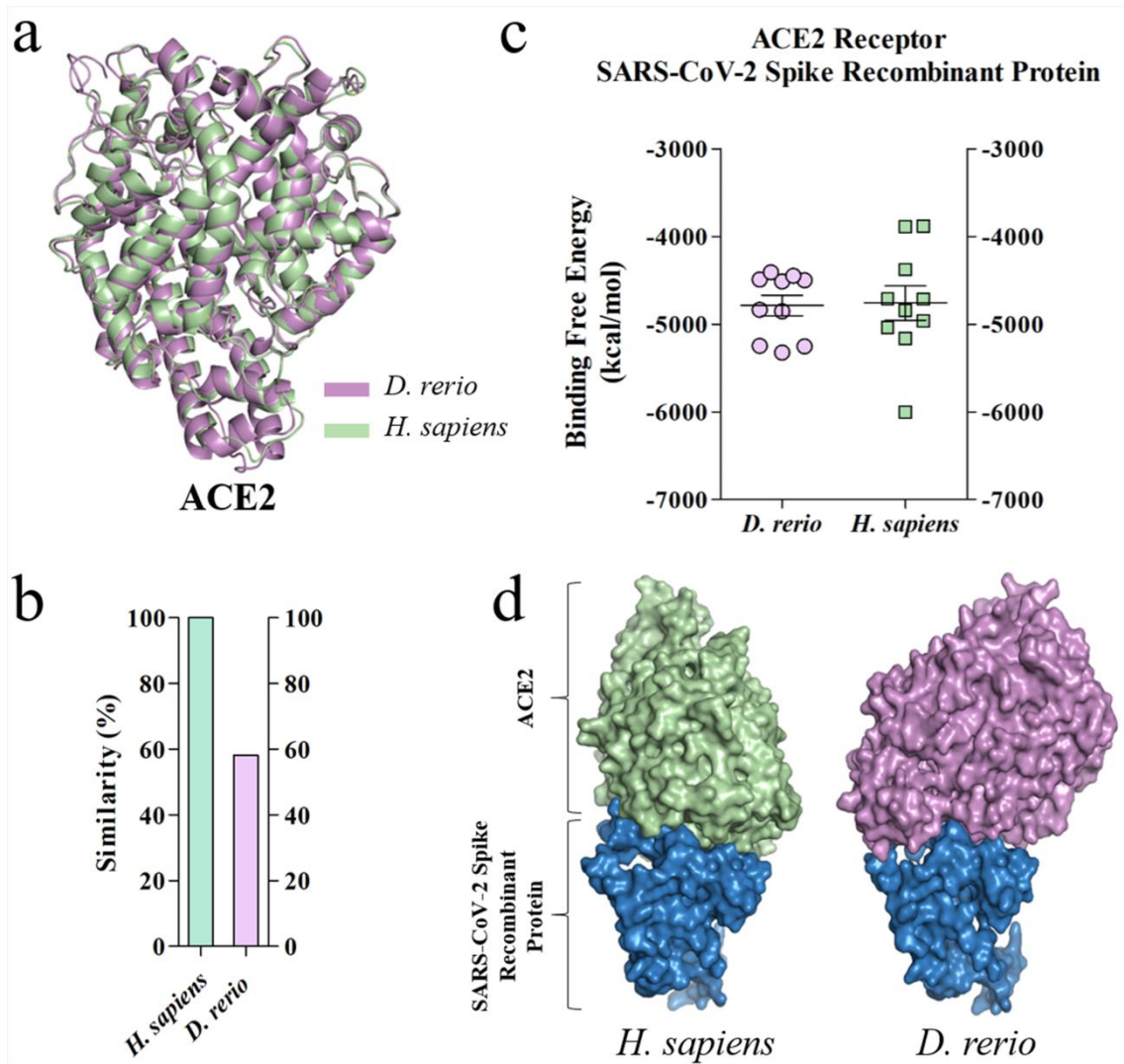


Figure 7

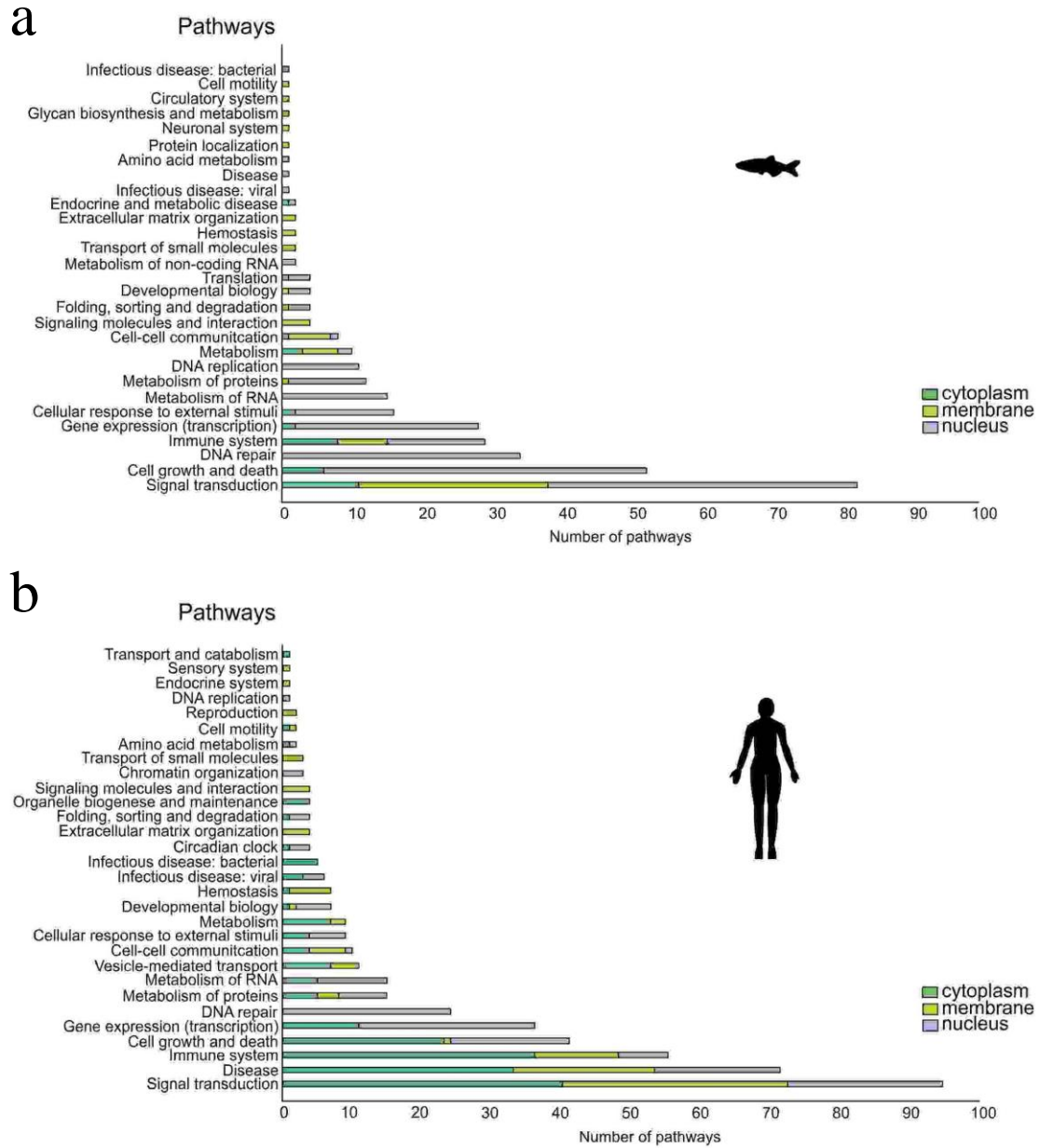
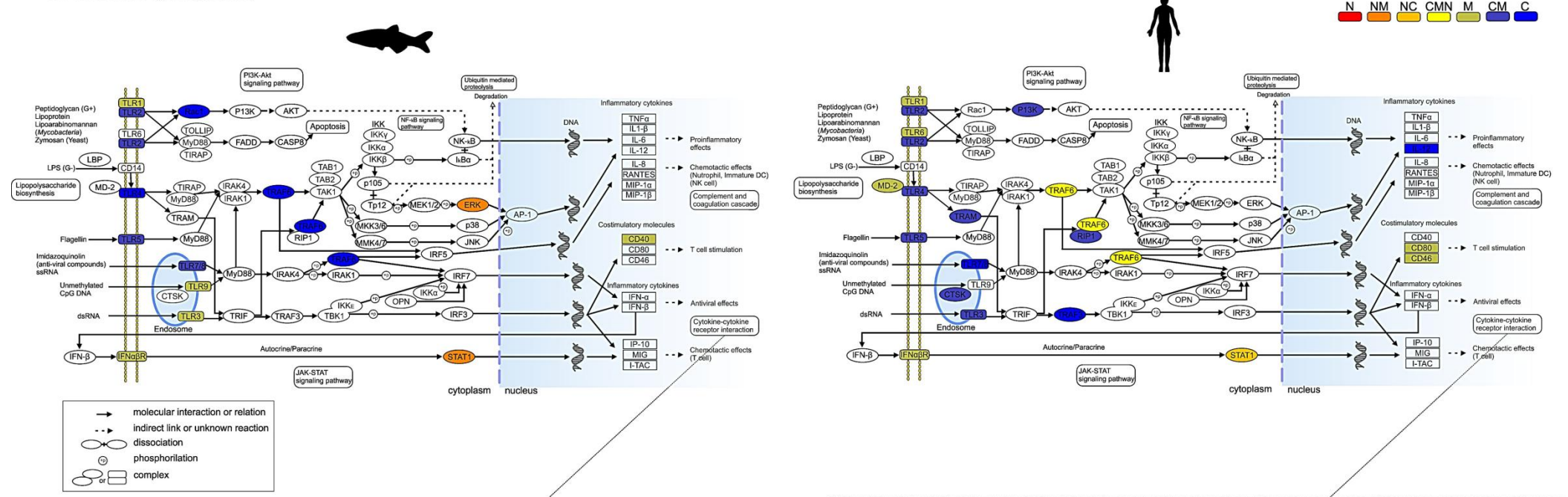
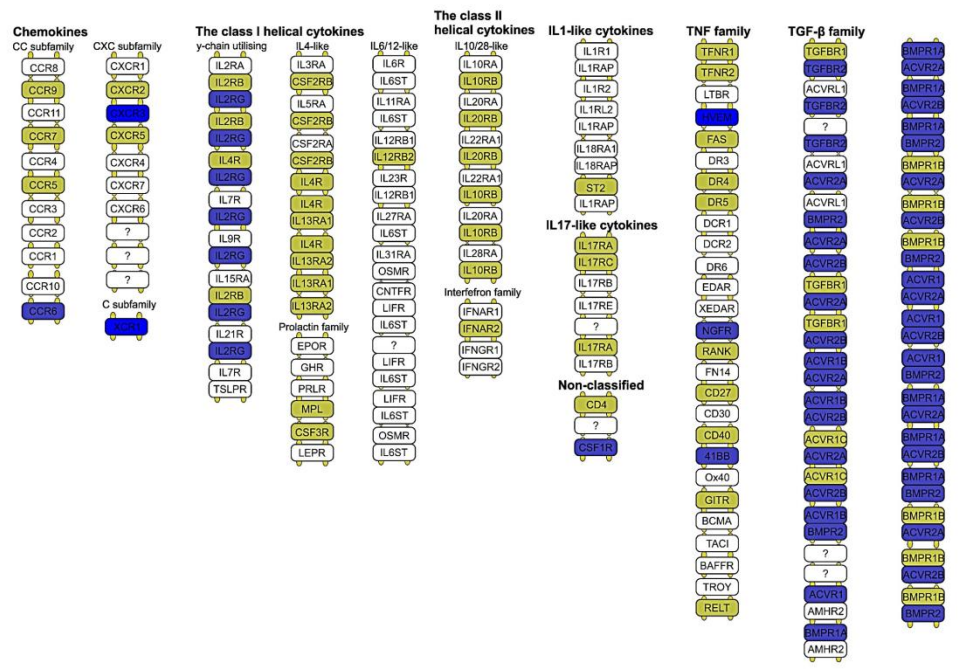


Figure 8

Toll-like receptor signaling pathway



Cytokine-cytokine receptor interaction



Cytokine-cytokine receptor interaction

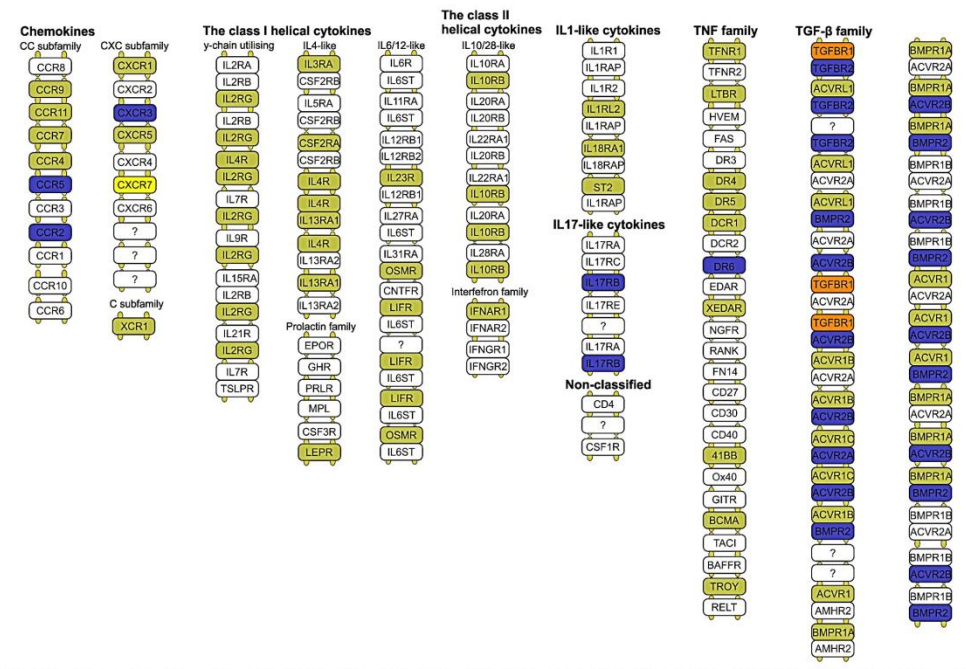


Figure 9

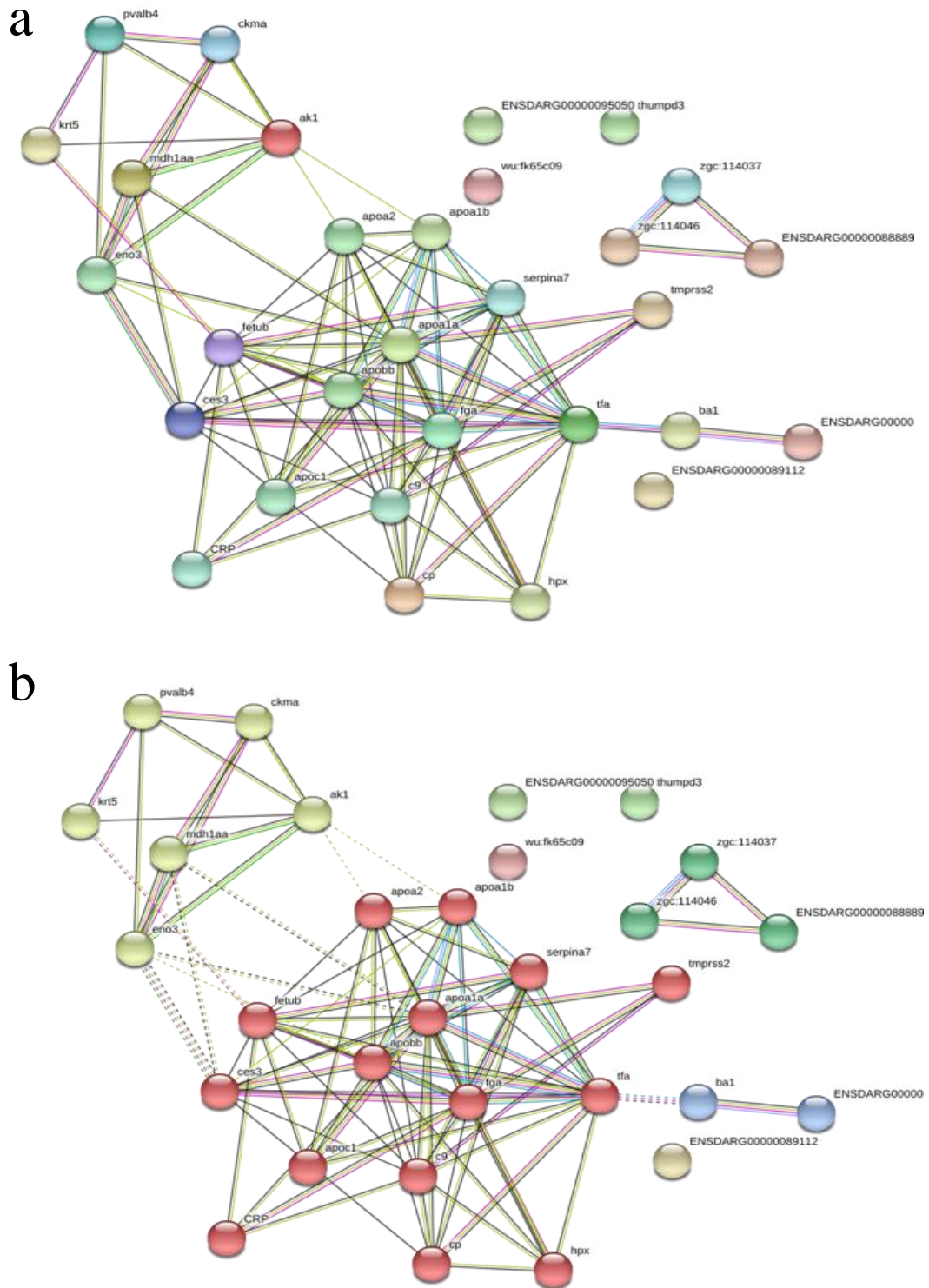


Figure 10

